Identification and characterization of novel factors in the DNA damage response

Singh, J.K.

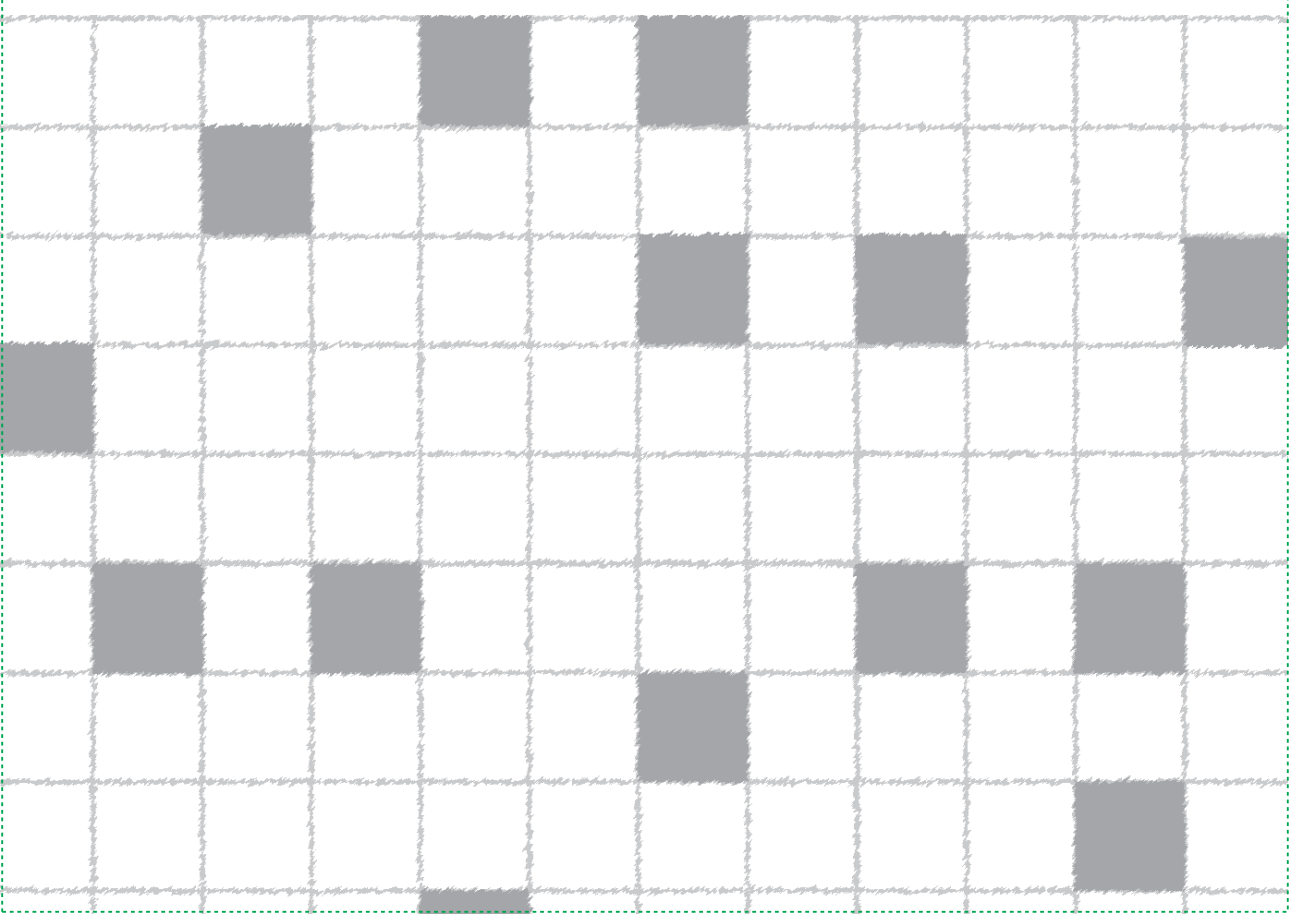

CHAPTER 5

Characterization of the exonuclease ERI1 in replication fork stability and R-loop formation

Jenny Kaur Singh, Wouter W. Wiegant, Magdalena B. Rother, Jolanthe Lingeman, Kees Vreeken, Anton J.L. de Groot, Román González-Prieto, Alfred C.O. Vertegaal, and Haico van Attikum.

ABSTRACT

The DNA in our cells is particularly vulnerable in S-phase, as many types of endogenous and exogenous sources can cause lesions that block replication fork progression and impact cell division. It is therefore essential for cells to activate replication stress pathways that stabilize and rescue stalled replication forks, allowing the completion of faithful DNA replication. Here, we describe the RNA processing factor ERI1 to play a role in the replication stress response. ERI1 depletion causes an increase in the levels of DNA-RNA hybrids (R-loops), which may enhance replication fork stalling and collapse. Indeed, ERI1 knockdown cells display increased phospho-RPA (S4/S8) levels after hydroxyurea (HU), which is indicative of replication fork instability. Accordingly, we found that ERI1 loss renders cells hypersensitive to HU-induced replication fork damage. Finally, we found that ERI1 is recruited to (stalled) replication forks, suggesting that ERI1 plays a direct role in the replication stress response. Future research will investigate how ERI1 functions at stalled replication forks and whether its function at these structures relies on its role in RNA-processing.

Keywords: Replication stress (RS), R-loops, ERI1, RNA processing

INTRODUCTION

DNA replication is a tightly regulated process in which the replisome rapidly copies billions of DNA bases during each cell division. This process is, however, constantly challenged by replication stress (RS) [1], which is defined as the slowing or stalling of replication fork progression and/or DNA synthesis, and can be caused by a multitude of impediments including limiting nucleotides, ribonucleotide incorporation, repetitive DNA elements, transcription-replication conflicts, DNA secondary structures, fragile sites, and oncogene-induced stress [2]. Fortunately, cells have evolved sophisticated S-phase and mitotic checkpoint pathways that help DNA replication to complete upon RS. Defects in these checkpoint pathways can lead to the stalling or collapse of replication forks, which in turn can cause mutations, chromosome rearrangements or the missegregation of chromosomes, thereby contributing to the development of diseases such as cancer [1].

ATR is the major kinase involved in dealing with RS. It is is recruited to RPA-coated single-stranded DNA (ssDNA) generated by uncoupling of the replicative MCM helicase from DNA polymerases at stalled replication forks, or for instance at replication-dependent DSBs induced by the topoisomerase I inhibitor camptothecin (CPT) [3, 4]. This is followed by its activation via two parallel pathways mediated by either ETAA1 or TOPBP1. ETAA1 stimulates ATR signaling by binding RPA on ssDNA, whereas TOPBP1 does so via its interaction with the RAD17 and 9-1-1 complexes at single-strand/double-strand DNA junctions [5, 6]. Once activated, ATR phosphorylates a wide variety of substrates, including CHK1 [7]. ATR-CHK1 then promote the restart of stalled replication forks, while enabling the slowdown or arrest of cell cycle progression until replication is completed [2], and controlling the firing of new origins to preserve the RPA pool [3]. Another failsafe mechanism that ensures fork integrity is replication fork reversal. During this process, annealing of newly synthesized and parental DNA occurs to form a fourth regressed arm, which becomes actively converted into a Holliday junction (HJ)-like structure [8]. Several key players are involved in fork reversal such as the SWI/SNF chromatin remodelers SMARCAL1 and ZRANB3, the helicase HLTF, as well as PARP1. PARP1 stabilizes reversed forks by inhibiting the activity of ATP-dependent DNA helicase Q1 (RECQ1), which can otherwise restart the fork [9]. Reversed forks are substrates for degradation by the nuclease MRE11 and must be properly protected by BRCA1, BRCA2 and Fanconi anemia (FA) proteins FANCA, FANCD2 and FANCJ to prevent fork collapse and ensure fork restart [10]. Alternatively, replication forks

that stall at DNA lesions can restart downstream of the lesion by PrimPol-dependent re-priming on the leading strand, leaving unreplicated ssDNA gaps to be filled post-replicatively by translesion synthesis (TLS) polymerases such as POL ɳ and REV1, or by template switching (TS), during which an undamaged homologous template on the sister chromatid is used to bypass DNA lesions [11].

Since DNA replication and transcription both utilize DNA, it is unavoidable that the two processes will interfere with each other, giving rise to transcription-replication conflicts (TRCs) [2]. TRCs can occur in a head-on (HO) or co-directional orientation (CD), depending on the orientation of the genes relative to the replication fork directionality. In mammalian cells the majority of replication forks progress through genes in a CD orientation to avoid the more deleterious HO collisions [12]. However, TRCs that occur in an HO orientation are frequently associated with the formation and persistence of R-loops. These are structures in which RNA is annealed to genomic DNA to create an RNA:DNA hybrid surrounded by a loop of non-templated single-stranded DNA which is protected by RPA [13, 14]. While R-Loops have several regulatory and topological roles in genome regulation, their persistence and association with TRCs can cause replication-stress associated genome instability [15].

RNA binding proteins have emerged as important players in preventing R-loops and genome stability [16]. RnaseH1 and RNaseH2 are evolutionary conserved enzymes that specifically degrade the RNA in R-loops. In addition, RNaseH2 removes single ribonucleotides mis-incorporated during DNA replication [17]. Interestingly, studies have implicated several other RNA processing factors in R-loop associated genome instability. For instance, the THO/TREX complex functions in transcription elongation and mRNP biogenesis to prevent the accumulation of R-loops [18], whereas SRSF1, a protein involved in RNA metabolism, is recruited to nascent transcripts by RNA polymerase II and prevents the formation of mutagenic R-loops [19]. However, despite several studies linking RNA binding proteins to R-loops and genome instability, the function of many RNA binding proteins in R-loop processing remains uncharacterized.

Here, we describe an important regulatory role of the exonuclease ERI1 in preventing R-loop formation following replication stress. ERI1 was found to be enriched at (stalled) replication forks and protects cells against replication stress. Our results suggest that ERI1 may resolve R-loop induced TRCs that lead to replication fork stalling and/or collapse.

RESULTS

ERI1 was among the candidate genes found whose loss causes sensitivity to Hydroxyurea (HU) treatment, which induced RS by dNTP depletion (Fig. 1A and [20]. To validate this finding, we performed clonogenic cell survival assays in the presence and absence of HU. We found that ERI1 loss rendered cells sensitive to HU, an effect that was similar to that observed after depletion of RPA-interacting protein ETAA1 (Fig. 1B and Fig. S1A [5]. To better understand how the absence of ERI1 sensitizes cells to replication stress (RS), we examined whether ERI1 is involved in ATR signaling following HU-induced helicase-polymerase uncoupling. ATR is the major kinase, which preserves the nuclear RPA pool by restraining the firing of new origins in order to prevent replication for instability. Inhibition of ATR in HU-treated cells leads to excessive double-strand break (DSB) formation and RPA hyperphosphorylation [3]. We found that ERI1-depleted cells showed increased levels of RPA2 phosphorylation at Serine 4 and 8 (p-RPA (S4/8) and Fig. 1C-D), as well as a mild increase in γH2AX levels (Fig. 1E). Interestingly, we also observed an increase in p-RPA (S4/8) levels upon camptothecin (CPT) treatment, which induces replication-dependent DSBs (Fig. S1B). Importantly, RPA levels remained unchanged in HU-treated ERI1-depleted cells (Fig. S1C-D). Finally, we employed the Flp-In/T-Rex system to establish U2OS cells stably expressing inducible and siRNA-resistant GFP-tagged ERI1 (Fig. 1F). Confirming our previous data (Fig. 1D), we found that ERI1 knockdown resulted in an increase of p-RPA (S4/8). Importantly, expression of siRNA-resistant GFP-ERI1 almost fully rescued the increase in p-RPA (S4/S8) observed after ERI1 knockdown (Fig. 1G-H), ruling out off-target effects of the siRNA against ERI1. Taken together, these results suggested that ERI1 protects cells against HU-induced RS likely by promoting replication fork stability.

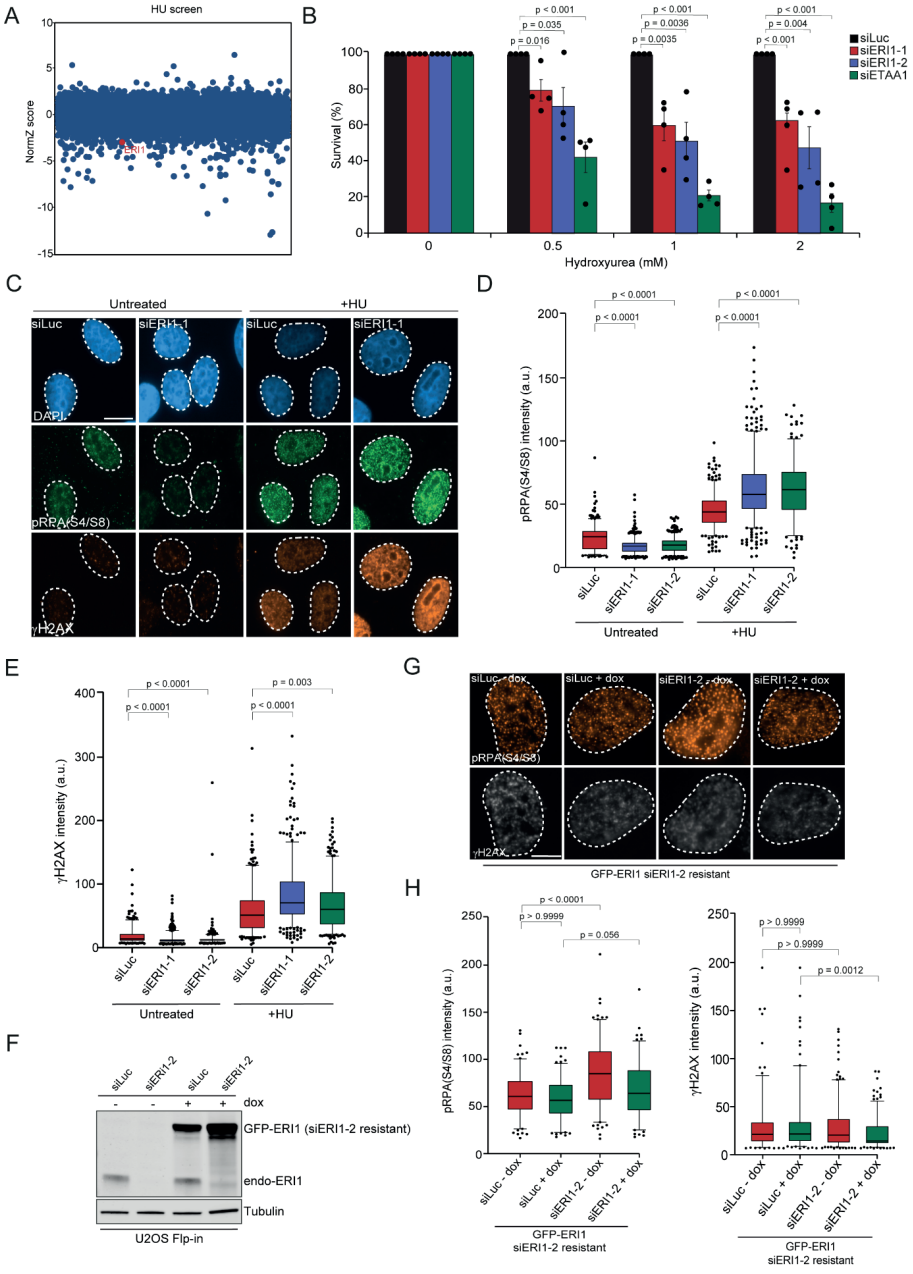
A
HU screen
NormZ score
ERI1
B
Survival (%)
Hydroxyurea (mM)
siLuc
siERI1-1
siERI1-2
siETAA1
p < 0.001
p = 0.035
p = 0.016
p = 0.0036
p = 0.0035
p = 0.004
C
Untreated
+HU
siLuc
siERI1-1
DAPI
pRPA(S4/S8)
γH2AX
D
pRPA(S4/S8) intensity (a.u.)
p < 0.0001
Untreated
+HU
E
γH2AX intensity (a.u.)
p = 0.003
F
dox
GFP-ERI1 (siERI1-2 resistant)
endo-ERI1
Tubulin
U2OS Flp-in
G
siLuc - dox
siLuc + dox
siERI1-2 - dox
siERI1-2 + dox
GFP-ERI1 siERI1-2 resistant
H
p > 0.9999
p = 0.056
p = 0.0012
GFP-ERI1
siERI1-2 resistant

► **Figure 1. ERI1 promotes cell survival and ATR signaling upon replication stress.** (A) CRISPR dropout screen results for RPE cells exposed to 2 mM HU. HU was added for 16 h every 3 days for a period of 12-14 days. (B) Relative survival efficiency in HCT116 cells transfected with the indicated siRNAs and treated with 0.5, 1 and 2 mM HU. The mean ±SEM of 3 independent experiments is shown. Data were normalized to un-irradiated conditions and set to 100%. Statistical significance was calculated using Student's *t* test. (C) Phosphorylated RPA at Ser4/8 and γH2AX foci formation in U2OS cells transfected with the indicated siRNAs. Cells were exposed to 2 mM of HU and foci intensity was measured after 4 hours. (D) Quantification of RPA (S4/8) foci intensity in cells from C. Mean foci intensity was quantified in immuno-stained p-RPA (S4/8) cells. The mean of 3 independent experiments is shown. (E) As in D, except that γH2AX foci intensity was measured. (F) Expression levels of endogenous ERI1 and dox-inducible siRNA-resistant GFP-ERI1 in U2OS Flp-In/TRex cells. Tubulin is a loading control. (G) Effect of inducible expression of siRNA resistant GFP-tagged ERI1 on phosphorylated RPA at Ser4/8 and γH2AX foci formation in U2OS cells transfected with the indicated siRNAs. Cells were exposed to 2 mM of HU and foci intensity was measured after 4 hours. (H) Quantification of RPA (S4/8) and γH2AX foci intensity in cells from G. Mean foci intensity was quantified in immuno-stained p-RPA (S4/8) and γH2AX cells. The mean of 3 independent experiments is shown. *P*-values were derived from Kruskal–Wallis ANOVA Dunn's post test.

ERI1 interacts with PARP1

To gain insight into ERI1's potential role in maintaining fork stability, we aimed to identify possible interaction partners of ERI1. To this end, we generated U2OS Flp-In/T-Rex cells stably expressing inducible GFP-tagged ERI1 or GFP-NLS, and performed GFP-trap-based pulldowns followed by label-free mass spectrometry (MS) (Fig. 2A). Our analysis revealed that ERI1 interacts with 173 proteins that were at least 2-fold enriched in GFP-ERI1 pulldowns when compared to those of GFP-NLS (Fig. 2A and Table S1). Although the majority of the interactors were ribosomal proteins, we also found additional interaction partners including RNA binding proteins (RNPS1 and PNN), RNA helicases (DHX15), chromatin remodelers (SMARCA5 and CHD4), histone proteins (HP1BP3, H1F0 and H2AFY) and RNA splicing factors (THRAP3). Interestingly, we found that ERI1 interacts with PARP1, a protein that is implicated in replication fork reversal [21], and TOP2A, a DNA topoisomerase involved in DNA replication [22]. Since ERI1 maintains fork integrity upon RS, we also performed the interaction analysis of GFP-ERI1 in the presence of HU and compared it to that of untreated cells (Fig. 2C and Table S1). In this analysis we found that ERI1 interacts with DHX9, a protein that recruits BRCA1 to RNA to promote DNA end-resection and homologous recombination (HR) repair [23]. Moreover, GNL3, a protein involved in the RS response, was also found to interact with ERI1 under these conditions [24]. Since PARP1 has several roles in the stabilization of stalled replication forks including fork reversal and the regulation of replication fork speed [25], we sought to validate this interaction. GFP pulldowns coupled to western blot analysis confirmed that GFP-tagged ERI1 interacts with endogenous PARP1 (Fig. 2B), manifesting a possible role of this interaction in RS.

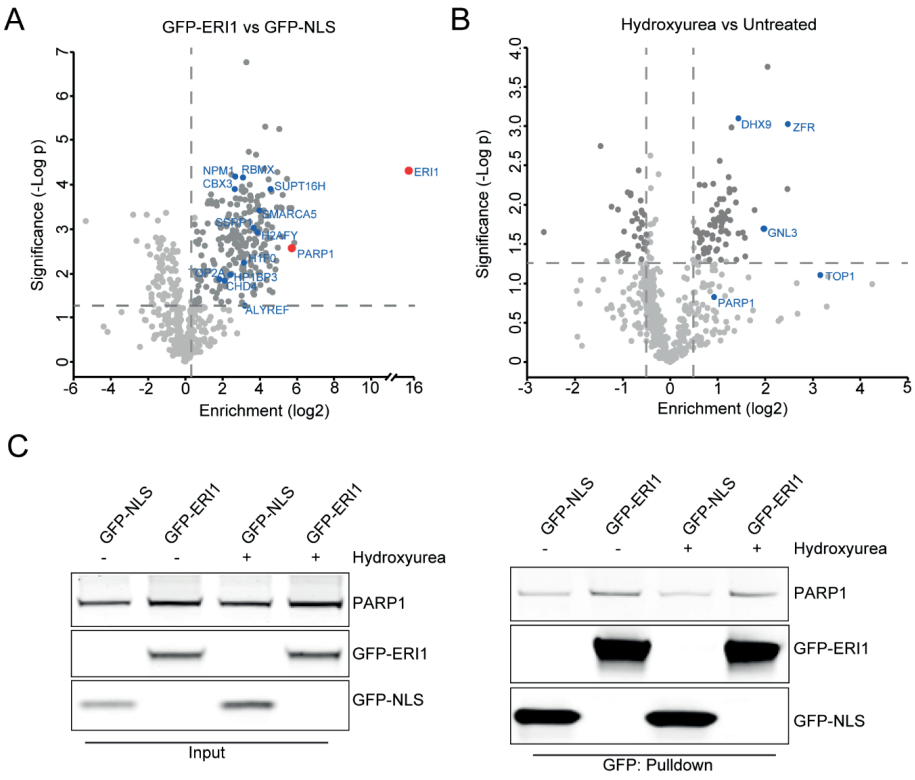

Figure 2. ERI1 interacts with PARP1. (A) Volcano plot depicting the statistical differences of the MS analysis on GFP-KANSL3 versus GFP-NLS pulldowns. The enrichment is plotted on the x-axis and the significance (t-test -log2 p-value) is plotted on the y-axis (see also Supplementary Table 1). (B) As in A, except that cells were treated with 2 mM HU for 4 hours before pulldowns. (C) Pull-down of the indicated GFP fusion proteins in the presence and absence of HU in U2OS Flp-In/T-Rex cells. Blots were probed for GFP and PARP1.

ERI1 is recruited to sites of DNA damage in a manner dependent on PARP activity

Next, we addressed whether ERI1 acts at sites of DNA damage induced by multi-photon laser micro-irradiation (Fig. 3A). Under these conditions, ectopically expressed GFP-tagged ERI1 co-expressed with the DNA damage sensor mCherry-NBS1 in U2OS cells, was rapidly recruited (within 30 s) to DNA damage tracks (Fig. 3B-C). Because of ERI1's interaction with PARP1, we analyzed whether it is recruited to sites of DNA damage via the activity of PARP. To this end, we treated cells with the PARP1 and PARP2 inhibitor (PARPi) Olaparib. This treatment almost completely abrogated the recruitment of GFP-

ERI1 (Fig. 2D-E). Thus, ERI1 is rapidly, but transiently recruited to sites of DNA damage in a manner dependent on the activity of PARP.

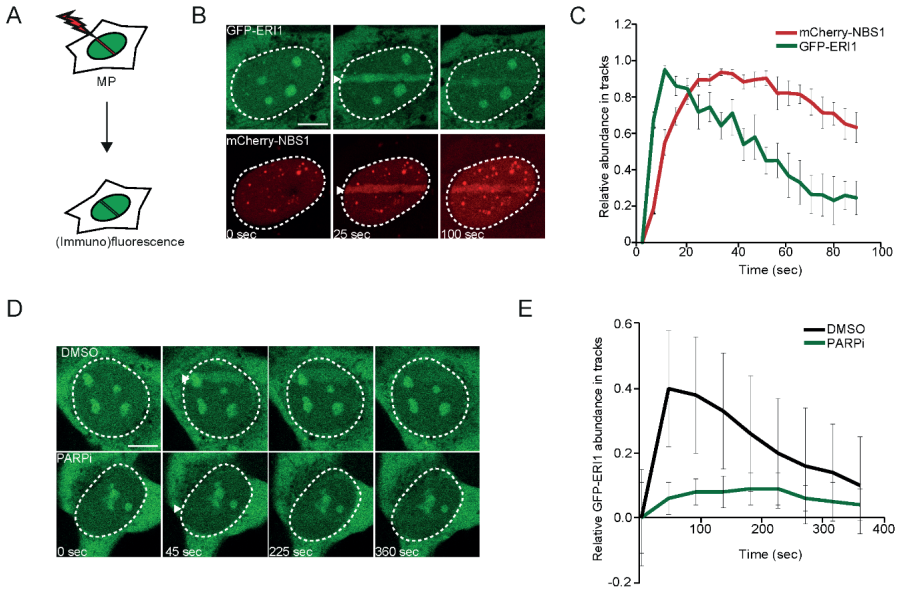

Figure 3. ERI1 is recruited to DNA damage sites via PAR/PARP. (A) Schematic representation of the laser micro-irradiation approach to study protein accumulation at sites of DNA damage. An 800 nm multiphoton (MP) laser was used. (B) Recruitment of GFP-ERI1 to 800 nm multiphoton tracks in U2OS Flp-In/T-Rex cells. mCherry-NBS1 was used as a DNA damage marker. White triangles indicate irradiated regions. (C) Quantification of B. The data are plotted on a timescale as relative abundance in tracks. Peak values were set to 1. The graph represents the mean ± SD of 2 independent experiments. (D) GFP-ERI1 recruitment to 800 nm multiphoton tracks in stable U2OS Flp-In/T-Rex cells treated with PARP inhibitor (PARPi) for 1 h before micro-irradiation. (E) Quantification of D. The data is presented as the mean ± SD.

ERI1 is enriched at (stalled) replication forks

Since multiphoton laser micro-irradiation may induce a variety of lesions other than damaged replication forks, we next investigated the presence of ERI1 on damaged forks [26]. We carried out the isolation of proteins on nascent DNA (iPOND) in unperturbed and replication stress conditions (Fig. 4A). Consistent with previous reports we observed an increase in replication stress proteins, including MRE11 and RPA phosphorylated at Serine 33 (Fig. 4B and [27]. Strikingly, we also found ERI1 enriched at unperturbed forks and increased at HU-induced stalled replication forks (Fig. 4B). This suggests that ERI1 associates with stalled replication forks to maintain their stability.

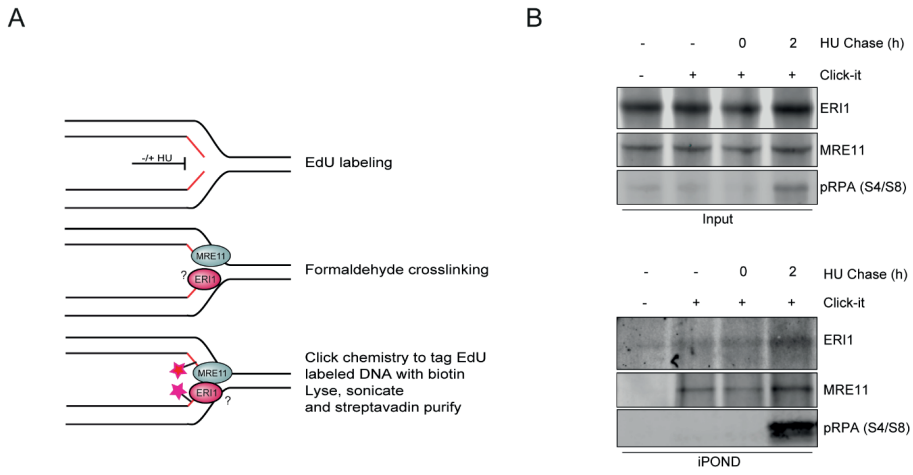

Figure 4. ERI1 is recruited to (stalled) replication forks. (A) Schematic representation of isolation of proteins on nascent DNA (iPOND) procedure. B) iPOND analysis of ERI1 in HEK293T cells after replication stress induced by 2mM HU for the indicated time points. Blots were probed for ERI1, MRE11 and p-RPA (S4/S8).

ERI1-depleted cells suffer from aberrant RNA-DNA hybrid formation

Given the role of ERI1 in several RNA-processing pathways [28], we hypothesized that ERI1 may be involved in the regulation of RNA-DNA hybrid structures (R-loops). R-loops are often associated with transcription-replication conflicts (TRCs), and might be responsible for the observed RS in ERI1-depleted cells. We therefore tested the impact of ERI1 on R-loop formation using the S9.6 antibody for immunofluorescence, which mostly recognizes R-loops, but also has low affinity for dsRNA structures [29]. In order to validate our S9.6 immunofluorescence staining, we depleted a well-known R-loop processing factor AQR and found, as expected, that this led to an increase in R-loop levels (Fig. S2A-B and [30]. In addition, we employed the Flp-In/T-Rex system to establish U2OS cells stably expressing inducible GFP-tagged RNaseH1 (Fig. S2C). Expression of GFP-RNaseH1 almost fully abolished R-loop formation, confirming the specificity of our S9.6 staining (Fig. S2D-E). Next, we measured the accumulation of R-loops in ERI1-depleted cells in both undamaged and CPT-treated cells. We found that loss of ERI1 increased the accumulation of R-loops most clearly following CPT treatment (Fig. 5A-C). Together, these results suggest that ERI1 suppresses R-loop formation, most prominently under RS conditions.

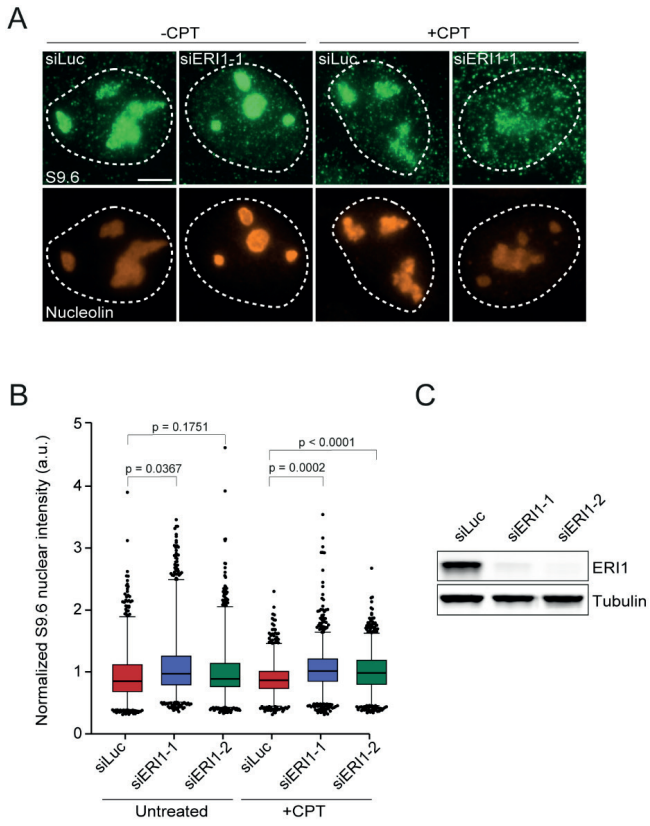

Figure 5. ERI1 suppresses the formation of R-loops. (A) S9.6 nuclear intensity was measured in U2OS cells transfected with the indicated siRNAs. Cells were exposed to 1 μM of CPT and foci intensity was measured after 2 hours. The S9.6 signal intensity per nucleus was determined by subtracting the S9.6 staining with that from nucleoli in each nucleus. (B) Quantification of S9.6 intensity in cells from A. Mean intensity was quantified in immuno-stained S9.6 cells. *P*-values were derived from Kruskal–Wallis ANOVA Dunn's post test. (C) Western blot analysis of ERI1 expression in cells from Figure 5A. Tubulin is a loading control.

The exonuclease domain of ERI1 is critical to suppress replication stress

Since ERI1 is a 3'exonuclease that possesses SAP and exonuclease domains required for binding and processing of RNA, respectively (Fig. 6A and [31, 32]. We next asked whether the decrease in fork stability as measured by phosphorylated RPA at Serine 4/8 relates to ERI1's role in RNA processing (Fig. 1D). Re-expression of siRNA-resistant GFP-tagged wildtype (Fig. 1G), but not exonuclease-dead (D130G and E132G) ERI1 largely suppressed p-RPA (S4/8) intensity in these cells (Fig. 6B-D and [33]. These data

suggest that replication fork stability is strictly dependent on the catalytic activity of ERI1. We speculate that ERI1 prevents the formation of TRCs by the resolution of R-loops and the subsequent stalling/collapse of replication forks (Fig. 6E).

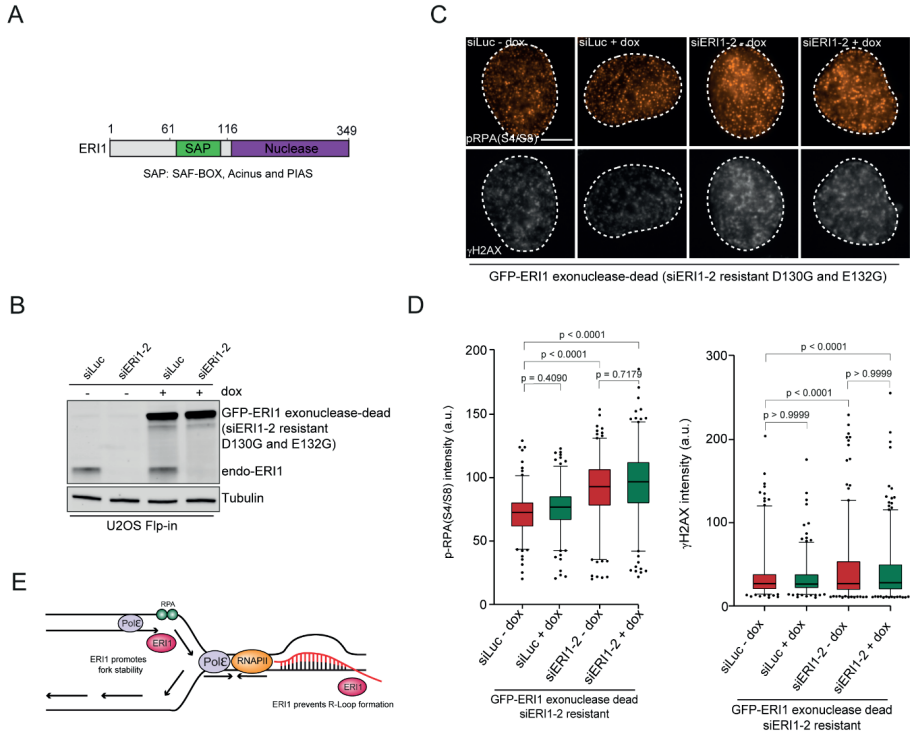

Figure 6. The catalytic activity of ERI1 is critical to suppress replication stress. (A) Schematic representation of full-length ERI1 protein with its indicated domains (SAP and nuclease domain). (B) Expression levels of endogenous ERI1 and dox-inducible siRNA-resistant GFP-ERI1 (exonuclease dead D130G and E132G) in U2OS Flp-In/TRex cells. Tubulin is a loading control. (G) Effect of inducible expression of siRNA resistant GFP-tagged ERI1 exonuclease dead on phosphorylated RPA at Ser4/8 and γH2AX foci formation in U2OS cells transfected with the indicated siRNAs. Cells were exposed to 2 mM of HU and foci intensity was measured after 4 hours. (H) Quantification of RPA (S4/8) and γH2AX foci intensity in cells from G. Mean foci intensity was quantified in immuno-stained p-RPA (S4/8) and γH2AX cells. The mean of 3 independent experiments is shown. *P*-values were derived from Kruskal–Wallis ANOVA Dunn's post test.

DISCUSSION

In this study, we uncover an important role of the exonuclease ERI1 in the RS response. First, we demonstrate that ERI1 protects cells from HU-induced RS and maintains fork stability under these conditions. Second, we show that ERI1 interacts with PARP1 and

is recruited to sites of DNA damage in a manner dependent on PARP activity. Third, iPOND analysis revealed that ERI1 associates with stalled replication forks. Finally, ERI1 suppresses the formation of R-loops and maintains fork stability through its activity in RNA-processing. Thus, ERI1 may ensure fork stability by preventing TRC collisions that are causally linked to R-loop formation and induce replication fork collapse (Fig. 6F).

ERI1 protects cells from HU-induced replication stress and maintains fork stability

In agreement with previous results we confirmed that ERI1-depleted cells are sensitive to HU-induced RS [20]. In response to HU-induced helicase-polymerase uncoupling, ATR kinase is recruited to and activated via its direct interaction with ssDNA at stalled replication forks [34]. This is followed by the ATR-dependent phosphorylation of RPA (at Serine 33), which prevents fork breakage by the suppression of new origin firing, thereby preserving the nuclear pool of RPA [3]. Consequently, inhibition of ATR leads to excessive amounts of ssDNA and limits the available amount RPA molecules by a process referred to as ´RPA exhaustion´. This phenomenon in turn leads to replication fork catastrophies and the formation of DSBs [5, 34]. RPA levels, however, remained unaffected in ERI1-depleted cells, ruling out RPA exhaustion. Instead, we found increased p-RPA (S4/S8) and γH2AX levels upon RS in ERI1-depleted cells. This suggests that ERI1 loss results in the conversion of stalled replication forks into collapsed forks, which may ultimately be converted into DSBs. To investigate this further, DNA fiber analysis may provide insights into whether ERI1 loss affects fork stability/recovery following replication stress.

ERI1 interacts with PARP1 and is enriched at (stalled) replication forks

Our mass spectrometry experiments revealed that the majority of ERI1 interactors are ribosomal proteins. However, we also found several additional interactors such as RNA binding proteins (RNPS1 and PNN), RNA helicases (DHX15), chromatin remodelers (SMARCA5 and CHD4), histone proteins (HP1BP3, H1F0 and H2AFY), RNA splicing factors (THRAP3) and the DNA repair protein PARP1 (Table S1). Moreover, we validated PARP1 as an ERI1 interactor by GFP-pulldowns coupled to western blot analysis, although this needs to be confirmed endogenously and reciprocally. Given that PARP1 is implicated in normal DNA replication and the stabilization of stalled replication forks, it may be possible that ERI1's role in these processes involves its interaction with

PARP1 [35]. Indeed, our findings reveal that ERI1 is recruited to sites of DNA damage via the activity of PARP. However, whether this involves the binding of ERI1 to PAR chains or to PARP1 itself needs to be further investigated [28]. Moreover, our iPOND analysis revealed that ERI1 is enriched at unperturbed forks and increased at HU-induced stalled replication forks. Similarly, PARP1 is activated and binds to HU-induced stalled replication forks [36]. Thus, it seems logical to next assess by iPOND whether ERI1's recruitment to stalled forks is dependent on PAR/PARP1. However, since ERI1 has affinity to bind RNA via its SAP domain, its recruitment to stalled forks may also rely on its interaction with RNA or its exonuclease activity (e.g. to process RNA in R-loops). Further work, including domain mapping analysis, should identify the PARP1 and RNA binding regions in ERI1 to resolve the functional relevance of interplay between ERI1 and PARP1 or RNA in response to replication fork stalling.

ERI1 depletion results in increased R-Loop formation

Our data reveal that ERI1 depletion leads to increased R-loop levels mostly following RS. We used the S9.6 antibody for immunofluorescence (IF) to measure R-loop levels. As expected, we found AQR depletion to increase the formation of R-loops, and overexpression of RnaseH1 to decrease the formation of R-loops, which validates our S9.6 IF [37]. However, because the S9.6 antibody also recognizes double-strand RNA [30, 38], it is of utmost importance to further validate our S9.6 IF experiments using RnaseIII treatment, as well as treatment with recombinant wildtype and catalytic inactive version of human RNaseH1 to further validate the specificity of our S9.6 IF [38]. Since ERI1 is involved in the processing of multiple RNA species [28], and our data reveal that the exonuclease domain of ERI1 is critical to suppress RS as measured by p-RPA (S4/8), it may be interesting to investigate whether the exonuclease domain of ERI1 has affinity to process the RNA in R-loops. Future *in vitro* R-loop formation assays using purified ERI1 wildtype and exonuclease dead will determine whether ERI1 processes R-loops and if this is dependent on its exonuclease domain [39].

The unscheduled formation of R-loops has been linked to TRCs and RS [40]. This raises the question whether the aberrant R-loops observed in ERI1-depleted cells, are a potential mechanism driving RS. Future endeavors including RNaseH1 overexpression rescue experiments in ERI1-depleted cells will give insight into whether the increase in fork stalling measured by p-RPA (S4/8) and DNA breaks measured by γH2AX levels, as well as the HU-sensitivity observed in ERI1-depleted cells is caused by R-loops.

Furthermore, R-loops may pose an obstacle for replication fork progression and thereby cause defects in replication fork instability upon HU-induced RS in ERI1-depleted cells [41]. To investigate this possibility, proximity ligation assay (PLA) between PCNA, as a marker for replication, and RNAPII may evaluate the occurrence of TRCs in absence of ERI1 [42].

A proper balance of histones and DNA during DNA replication is crucial, as dysregulation of the amount of histone levels is associated with chromosomal loss and genome instability [43]. ERI1 is required for the degradation of replication-dependent histone mRNAs [44, 45]. This raises the question whether this function of ERI1 is linked to R-loops and is associated replication stress. It would be important to decipher the genomic location in which R-loops are enriched in ERI1 depleted cells, and whether this correlates with changes in histone incorporation levels at these loci during replication. In depth analysis of R-loop distribution by DRIP-sequencing in both control and ERI1-depleted cells, as well as ChIP-sequencing, including e.g. chromatin occupancy after replication-seq (ChOR-seq) [46], to determine changes in histone levels at these sites will be required in the future to address these questions.

MATERIAL AND METHODS

Cell lines

U2OS and HCT116 cells were cultured in 5% CO_2 at 37°C in DMEM (Dulbecco's modified Eagle's medium) supplemented with 10% fetal calf serum and antibiotics. U2OS Flp-In/T-Rex cells, which were generated using the Flp-In/T-REx system (Thermo Fisher Scientific), were a gift of Geert Kops (University Medical Center Utrecht, the Netherlands) and Stephen Taylor (University of Manchester, UK). These cells were used to stably express inducible versions of GFP-NLS, as well as GFP-ERI1 by co-transfection of pCDNA5/FRT/TO-Puro plasmid encoding GFP or GFP-tagged ERI1 (5 μg), together with pOG44 plasmid encoding the Flp recombinase (1 μg). After selection on 1 μg/mL puromycin, single clones were isolated and expanded. U2OS Flp-In/T-Rex were incubated with 2 μg/mL doxycycline for 24h to induce expression of cDNAs. All cells were authenticated by STR profiling and tested negative in routinely performed mycoplasma tests.

Chemicals

Cells were treated with 2mM Hydroxyurea (Sigma) at the indicated timepoints and collected for further analysis. The PARP inhibitor olaparib (Selleck Chemicals) was used at a final concentration of 10 μM. Camptothecin (Sigma-Aldrich) was used at a final concentration of 1 μM.

Transfections, siRNAs and plasmids

Cells were transfected with siRNAs using RNAiMAX (Invitrogen) according to the manufacturer's instructions. Cells were transfected twice with siRNAs at 0 and 24 h at a concentration of 40 nM and were analyzed 48 h after the second transfection unless otherwise indicated. siRNA sequences are listed in Table 1. Cells were transfected with plasmid DNA using Lipofectamine 2000 (Invitrogen) according to the manufacturer's instructions and analyzed 24-48 hours after transfection. The expression vector for full length human ERI1 (ORFeome collection), was amplified and cloned into pCDNA5/FRT/TO-Puro as a *BspEI/Acc65I* fragment (Table 2). Mutant constructs were generated by site-directed mutagenesis PCR (Table 2). siERI1-resistant cDNA was generated by introducing the underlined mutations GTTATCGATTGGATGAAGTTA by overlap PCR and cloned as *BspEI/Acc65I* fragment into pCDNA5/FRT/TO-Puro-ERI1-WT (Table 2). All ERI1 expression constructs were verified using Sanger sequencing.

Multiphoton laser micro-irradiation

Cells grown were grown on 18 mm coverslips. For micro-irradiation, cells were placed in a Chamlide CMB magnetic chamber and the growth medium was replaced by CO_2-independent Leibovitz's L15 medium supplemented with 10% FCS and antibiotics. Laser micro-irradiation was performed on a Leica SP5 confocal microscope equipped with an environmental chamber set to 37°C. DNA damage-containing tracks (1.5 μm width) were generated with a Mira mode locked titanium-sapphire (Ti:Sapphire) laser (l = 800 nm, pulse length = 200 fs, repetition rate = 76 MHz, output power = 80 mW) using a UV-transmitting 63x 1.4 NA oil immersion objective (HCX PL APO; Leica). Confocal images were recorded before and after laser irradiation at 5 seconds time interval over a period of 3-5 minutes. Images after multi-photon micro-irradiation of living cells were recorded using LAS-AF software (Leica) and analyzed with Image J as described previously [47]. The average pixel intensity of laser tracks was measured within the locally irradiated area (Idamage), in the nucleoplasm outside the locally irradiated area (Inucleoplasm)

and in a region not containing cells in the same field of view (Ibackground). The level of protein accumulation relative to the protein level in the nucleoplasm was calculated as follows: ((Idamage – Ibackground)/(Inucleoplasm – Ibackground) – 1).

Immunofluorescence analysis

Cells were either directly fixed with 2% formaldehyde in PBS for 20 minutes at room temperature (RT), or pre-extracted with 0.5% Triton-X100 (Serva) in PBS on ice for 2-5 minutes prior to fixation. Alternatively, cells were fixed, post-extracted with 0.25% Triton-X100 (Serva) in PBS and treated with 100 mM glycine in PBS for 20 minutes to block unreacted aldehyde groups. Cells were then rinsed with PBS and equilibrated in wash buffer (PBS containing 0.5% BSA). Antibody incubation steps and washes were in wash buffer. Primary antibodies were incubated for 1-2 hours at room temperature. Detection was done using goat anti-mouse or goat anti-rabbit Ig coupled to Alexa 488, 555 or 647 (1:1500; Invitrogen Molecular probes). All antibodies are listed in Table 3. Samples were incubated with 0.1 μg/mL 4',6-Diamidino-2-Phenylindole Dihydrochloride (DAPI) and mounted in Polymount.

Sample preparation and mass spectrometry

For mass spectrometry, U2OS Flp-In/T-Rex cells expressing GFP-NLS and GFP-ERI1^{WT} were treated with 2 mM Hydroxyurea for 4 hours or left untreated. Cell pellets were lysed in EBC-1 buffer (50 mM Tris, pH 7.5, 150 mM NaCl, 0.5% NP-40, 2 mM $MgCl_2$, protease inhibitor cocktail tablets) with 500 units benzonase. Samples were incubated for 1 hour at 4°C under constant mixing followed by high speed centrifugation for 10 minutes at 4°C. Protein concentration was measured by Qubit in the cleared lysates, equalized and transferred to tubes containing GFP-Trap beads (Chromotek). After 90 minutes of incubation at 4°C under rotating condition, the beads were washed 4 times with EBC-2 buffer (50 mM Tris pH 7.5, 150 mM NaCl, 1 mM EDTA, and protease inhibitor cocktail tablets) and 3 times with 50 mM ammonium bicarbonate followed by overnight digestion using 2.5 μg trypsin at 37°C under constant shaking. Digestion was terminated with 1% trifluoroacetic acid and centrifuged for 5 minutes at high speed to precipitate insoluble fractions. Consequently, C18 cartridges were prepared by washing 2 times with acetonitrile followed by 2 times with 0,1% Acetic acid. Peptides were loaded on the cartridge, while bound peptides were washed 2 times with 0.1% acetic acid and eluted with 1 mL 80% acetonitrile / 0.1% acetic acid and lyophilized.

Mass spectrometry was performed essentially as previously described [48]. Samples were nalysed on a Q-Exactive Orbitrap mass spectrometer (Thermo Scientific, Germany) coupled to an EASY-nanoLC 1000 system (Proxeon, Odense, Denmark). Digested peptides were separated using a 15 cm fused silica capillary (ID: 75 µm, OD: 375 µm, Polymicro Technologies,California, US) in-house packed with 1.9 µm C18-AQ beads (Reprospher-DE, Pur, Dr. Maisch, Ammerburch-Entringen, Germany). Peptides were separated by liquid chromatography using a gradient from 2% to 95% acetonitrile with 0.1% formic acid at a flow rate of 200 nl/minute for 65 minutes. The mass spectrometer was operated in positive-ion mode at 2.8 kV with the capillary heated to 250°C, and in a Data-Dependent Acquisition (DDA) mode with a top 7 method. Full scan MS spectra were obtained with a resolution of 70,000, a target value of $3x10^6$ and a scan range from 400 to 2,000 m/z. Maximum Injection Time (IT) was set to 50 ms. Higher-Collisional Dissociation (HCD) tandem mass spectra (MS/MS) were recorded with a resolution of 35,000, a maximum IT of 20 ms, a target value of $1x10^5$ and a normalized collision energy of 25%. The precursor ion masses selected for MS/MS analysis were subsequently dynamically excluded from MS/MS analysis for 60 seconds. Precursor ions with a charge state of 1 and greater than 6 were excluded from triggering MS/MS events. Three replicates were included per condition with two technical repeats each.

Mass Spectrometry data analysis

Raw mass spectrometry files were analysed with MaxQuant software (v1.5.3.30) as described [49] with the following modifications from default settings: the maximum number of mis-cleavages by trypsin/p was set to 3, Label Free Quantification (LFQ) was enabled disabling the Fast LFQ feature. Match-between-runs feature was enabled with a match time window of 0.7 minutes and an alignment time window of 20 minutes. We performed the search against an in silico digested UniProt reference proteome for Homo sapiens (8^{th} June 2020). Analysis output from MaxQuant was further processed in the Perseus (v 1.5.5.3) computational platform [49]. Proteins identified as common contaminants, only identified by site and reverse peptide, were filtered out, and then all the LFQ intensities were log2 transformed. Different biological repeats of each condition were grouped and only protein groups identified in all three biological replicates in at least one condition were included for further analysis. Missing values were imputed using Perseus software by normally distributed values with a 1.8 downshift (log2) and a randomized 0.3 width (log2) considering total matrix values. Volcano plots were

generated, and Student's T-tests were performed to compare the different conditions. Spreadsheets from the statistical analysis output from Perseus were further processed in Microsoft Excel for comprehensive visualization and analysis of the data (Table S1).

Western blot analysis

Cells were lysed in 2x Laemmli buffer and proteins were separated by Sodium Dodecyl Sulfate PolyAcrylamide Gel Electrophoresis (SDS-PAGE) using 4-12% pre-cast polyacrylamide gels (BioRad or Invitrogen) and MOPS running buffer (Invitrogen). Next, proteins were transferred onto nitrocellulose membranes (Millipore). Protein expression was analyzed by immunoblotting with the indicated primary antibodies (Table 3) and secondary CF680 goat anti-rabbit or CF770 goat anti-mouse Ig antibodies (1:5000, Biotium). Membranes were scanned and analyzed using a Licor Odyssey scanner (LI-COR Biosciences).

Isolation of proteins on nascent DNA (iPOND)

iPOND was performed as described by [27] with minor modifications. Briefly, 80-100*10^6 HEK293T cells were pulse labelled with 10 μM 5-ethynyl-2'-deoxyuridine (EdU; Invitrogen) for 20 min. Next, cells were treated with 2 mM HU for 5 hr to induce stalled forks. After treatment, cells were cross-linked with 1% formaldehyde without methanol in PBS for 15 min at room temperature, quenched with 0.125 M glycine and collected by scraping. Fixed cells were spun down for 5 min at 4 ˚C and 900 g, washed two times with PBS. Next, cells were permeabilized with 0.25% Triton X-100 in PBS for 30 min at room temperature, followed by incubation with click-iT reaction buffer (10 μM biotin azide (life technologies), 10 mM sodium-L-ascorbate, and 2 mM $CuSO_4$) or control buffer for 3 hr at room temperature. The cells were then washed with 0.5% BSA/PBS, and resuspended in lysis buffer (0.5% SDS, 50 mM Tris-HCl pH 8.0, protease inhibitors (Roche)). Samples were then sonicated using a Branson 250 SONIFIER with microtip for 1 s pulse for 10 cycles, repeated 3 times, with 90 s pause between repetition. For input samples, an aliquot of the lysate was taken. The rest of the samples were incubated with pre-washed streptavidin coated beads (Life Technologies) for 1 hr at room temperature. Beads were washed twice with high salt buffer (1% Triton X-100, 20 mM Tris [pH 8.0], 2 mM EDTA, 500 mM NaCl) and twice with lithium chloride salt wash buffer (100 mM Tris [pH 8.0], 500 mM LiCl and 1% Igepal [NP-40]), followed by elution of the captured proteins by boiling the beads in 2X Laemmli for 25 min at 95˚C. Proteins were separated on a 4-12% Criterion™ XT Bis-Tris gel (Bio-Rad) and detected by western blot.

Cell survival assays

HCT116 cells were transfected with siRNAs, trypsinized, seeded at low density and exposed to HU for 24 hours. For HCT116 Flp-In/T-Rex, cDNAs were expressed by adding Dox for 24 hours after siRNA transfection. After 12 days, the cells were washed with 0.9% NaCl and stained with methylene blue (2.5 g/L in 5% ethanol, Sigma-Aldrich). Colonies of more than 20 cells were scored.

AUTHOR CONTRIBUTION

J.S. performed western blot analysis, immunofluorescence experiments, clonogenic survival assays. J.L. and W.W.W. performed iPOND assay. A.J.L.G. prepared mass-spectrometry samples. R.P. and A.C.O.V. performed mass-spectrometry experiments and data analysis. H.v.A. conceived and supervised the project.

ACKNOWLEDGEMENTS

We thank Niels Mailand for kindly providing valuable reagents. This research was financially supported by the European Research Council (ERC) under the European Union's Horizon 2020 research and innovation program (ERC-StG 310913 to A.C.O.V.; ERC-CoG 50364 to H.v.A)

REFERENCES

1. Gaillard, H., T. García-Muse, and A. Aguilera, *Replication stress and cancer.* Nature Reviews Cancer, 2015. **15**(5): p. 276-289.
2. Zeman, M.K. and K.A. Cimprich, *Causes and consequences of replication stress.* Nat Cell Biol, 2014. **16**(1): p. 2-9.
3. Toledo, L.I., et al., *ATR prohibits replication catastrophe by preventing global exhaustion of RPA.* Cell, 2013. **155**(5): p. 1088-103.
4. O'Connell, B.C., et al., *A genome-wide camptothecin sensitivity screen identifies a mammalian MMS22L-NFKBIL2 complex required for genomic stability.* Mol Cell, 2010. **40**(4): p. 645-57.
5. Haahr, P., et al., *Activation of the ATR kinase by the RPA-binding protein ETAA1.* Nature Cell Biology, 2016. **18**(11): p. 1196-1207.
6. Bass, T.E., et al., *ETAA1 acts at stalled replication forks to maintain genome integrity.* Nat Cell Biol, 2016. **18**(11): p. 1185-1195.
7. Zhao, H. and H. Piwnica-Worms, *ATR-mediated checkpoint pathways regulate phosphorylation and activation of human Chk1.* Molecular and cellular biology, 2001. **21**(13): p. 4129-4139.
8. Neelsen, K.J. and M. Lopes, *Replication fork reversal in eukaryotes: from dead end to dynamic response.* Nature Reviews Molecular Cell Biology, 2015. **16**(4): p. 207-220.
9. Berti, M., et al., *Human RECQ1 promotes restart of replication forks reversed by DNA topoisomerase I inhibition.* Nat Struct Mol Biol, 2013. **20**(3): p. 347-54.
10. Schlacher, K., H. Wu, and M. Jasin, *A distinct replication fork protection pathway connects Fanconi anemia tumor suppressors to RAD51-BRCA1/2.* Cancer Cell, 2012. **22**(1): p. 106-16.
11. Quinet, A., et al., *To skip or not to skip: choosing repriming to tolerate DNA damage.* Molecular Cell, 2021. **81**(4): p. 649-658.
12. Lin, Y.-L. and P. Pasero, *Transcription-Replication Conflicts: Orientation Matters.* Cell, 2017. **170**(4): p. 603-604.
13. Nguyen, H.D., et al., *Functions of Replication Protein A as a Sensor of R Loops and a Regulator of RNaseH1.* Mol Cell, 2017. **65**(5): p. 832-847.e4.
14. Gaillard, H. and A. Aguilera, *Transcription as a Threat to Genome Integrity.* Annu Rev Biochem, 2016. **85**: p. 291-317.
15. Crossley, M.P., M. Bocek, and K.A. Cimprich, *R-Loops as Cellular Regulators and Genomic Threats.* Mol Cell, 2019. **73**(3): p. 398-411.
16. Costantino, L. and D. Koshland, *The Yin and Yang of R-loop biology.* Current Opinion in Cell Biology, 2015. **34**: p. 39-45.
17. Hiller, B., et al., *Mammalian RNase H2 removes ribonucleotides from DNA to maintain genome integrity.* J Exp Med, 2012. **209**(8): p. 1419-26.
18. Gómez-González, B., et al., *Genome-wide function of THO/TREX in active genes prevents R-loop-dependent replication obstacles.* The EMBO journal, 2011. **30**(15): p. 3106-3119.
19. Li, X. and J.L. Manley, *Inactivation of the SR Protein Splicing Factor ASF/SF2 Results in Genomic Instability.* Cell, 2005. **122**(3): p. 365-378.
20. Olivieri, M., et al., *A genetic map of the response to DNA damage in human cells.* 2019: p. 845446.
21. Genois, M.-M., et al., *CARM1 regulates replication fork speed and stress response by stimulating PARP1.* Molecular Cell, 2021. **81**(4): p. 784-800.e8.

22. Nitiss, J.L., *DNA topoisomerase II and its growing repertoire of biological functions.* Nature Reviews Cancer, 2009. **9**(5): p. 327-337.
23. Chakraborty, P. and K. Hiom, *DHX9-dependent recruitment of BRCA1 to RNA promotes DNA end resection in homologous recombination.* Nature Communications, 2021. **12**(1): p. 4126.
24. Lin, T., et al., *Nucleostemin and GNL3L exercise distinct functions in genome protection and ribosome synthesis, respectively.* J Cell Sci, 2014. **127**(Pt 10): p. 2302-12.
25. Ray Chaudhuri, A. and A. Nussenzweig, *The multifaceted roles of PARP1 in DNA repair and chromatin remodelling.* Nature Reviews Molecular Cell Biology, 2017. **18**(10): p. 610-621.
26. Reynolds, P., et al., *Spatiotemporal dynamics of DNA repair proteins following laser microbeam induced DNA damage – When is a DSB not a DSB?* Mutation Research/Genetic Toxicology and Environmental Mutagenesis, 2013. **756**(1): p. 14-20.
27. Sirbu, B.M., et al., *Analysis of protein dynamics at active, stalled, and collapsed replication forks.* Genes Dev, 2011. **25**(12): p. 1320-7.
28. Thomas, M.F., N.D. L'Etoile, and K.M. Ansel, *Eri1: a conserved enzyme at the crossroads of multiple RNA-processing pathways.* Trends in genetics : TIG, 2014. **30**(7): p. 298-307.
29. Crossley, M.P., et al., *Catalytically inactive, purified RNase H1: A specific and sensitive probe for RNA-DNA hybrid imaging.* J Cell Biol, 2021. **220**(9).
30. Sollier, J., et al., *Transcription-Coupled Nucleotide Excision Repair Factors Promote R-Loop-Induced Genome Instability.* Molecular Cell, 2014. **56**(6): p. 777-785.
31. Yang, X.C., et al., *Characterization of 3'hExo, a 3' exonuclease specifically interacting with the 3' end of histone mRNA.* J Biol Chem, 2006. **281**(41): p. 30447-54.
32. Ansel, K.M., et al., *Mouse Eri1 interacts with the ribosome and catalyzes 5.8S rRNA processing.* Nat Struct Mol Biol, 2008. **15**(5): p. 523-30.
33. Cheng, Y. and D.J. Patel, *Crystallographic structure of the nuclease domain of 3'hExo, a DEDDh family member, bound to rAMP.* J Mol Biol, 2004. **343**(2): p. 305-12.
34. Liao, H., et al., *Mechanisms for stalled replication fork stabilization: new targets for synthetic lethality strategies in cancer treatments.* EMBO reports, 2018. **19**(9): p. e46263.
35. Ray Chaudhuri, A. and A. Nussenzweig, *The multifaceted roles of PARP1 in DNA repair and chromatin remodelling.* Nature reviews. Molecular cell biology, 2017. **18**(10): p. 610-621.
36. Bryant, H.E., et al., *PARP is activated at stalled forks to mediate Mre11-dependent replication restart and recombination.* The EMBO Journal, 2009. **28**(17): p. 2601-2615.
37. Sakasai, R., et al., *Aquarius is required for proper CtIP expression and homologous recombination repair.* Scientific Reports, 2017. **7**(1): p. 13808.
38. Crossley, M.P., et al., *Catalytically inactive, purified RNase H1: A specific and sensitive probe for RNA–DNA hybrid imaging.* Journal of Cell Biology, 2021. **220**(9).
39. Kasahara, M., et al., *RecA protein-dependent R-loop formation in vitro.* Genes & development, 2000. **14**(3): p. 360-365.
40. García-Muse, T. and A. Aguilera, *Transcription–replication conflicts: how they occur and how they are resolved.* Nature Reviews Molecular Cell Biology, 2016. **17**(9): p. 553-563.
41. Gómez-González, B. and A. Aguilera, *Transcription-mediated replication hindrance: a major driver of genome instability.* Genes Dev, 2019. **33**(15-16): p. 1008-1026.

42. Bayona-Feliu, A., et al., *The SWI/SNF chromatin remodeling complex helps resolve R-loop-mediated transcription–replication conflicts.* Nature Genetics, 2021.
43. Kaygun, H. and W.F. Marzluff, *Regulated degradation of replication-dependent histone mRNAs requires both ATR and Upf1.* Nat Struct Mol Biol, 2005. **12**(9): p. 794-800.
44. Hoefig, K.P., et al., *Eri1 degrades the stem-loop of oligouridylated histone mRNAs to induce replication-dependent decay.* Nat Struct Mol Biol, 2013. **20**(1): p. 73-81.
45. Hoefig, K.P. and V. Heissmeyer, *Degradation of oligouridylated histone mRNAs: see UUUUU and goodbye.* WIREs RNA, 2014. **5**(4): p. 577-589.
46. Reverón-Gómez, N., et al., *Accurate Recycling of Parental Histones Reproduces the Histone Modification Landscape during DNA Replication.* Mol Cell, 2018. **72**(2): p. 239-249.e5.
47. Luijsterburg, M.S., et al., *PARP1 Links CHD2-Mediated Chromatin Expansion and H3.3 Deposition to DNA Repair by Non-homologous End-Joining.* Mol Cell, 2016. **61**(4): p. 547-62.
48. Kumar, R., et al., *The STUbL RNF4 regulates protein group SUMOylation by targeting the SUMO conjugation machinery.* Nat Commun, 2017. **8**(1): p. 1809.
49. Tyanova, S., T. Temu, and J. Cox, *The MaxQuant computational platform for mass spectrometry-based shotgun proteomics.* Nat Protoc, 2016. **11**(12): p. 2301-2319.

Table 1. List of siRNAs

Target	Sequence (5'-3')
ERI1-1	ACGAAUGGCUGUAUUAAUA
ERI1-2	GUAAUUGACUGGAUGAAAU
XRCC4	AUAUGUUGGUGAACUGAGA
ETAA1	GAGCAAAACAAGAGGAAUUUU
Luciferase	CGUACGCGGAAUACUUCGA
AQR	SMARTpool (siGENOME)

Table 2. List of primers

Name	Sequence (5'-3')
HindIII FW	TAAAAAGCTTATATGGAAGAATCTCACTTCAATTCTAAC
KpnI RV	TAATAATGGTACCCTAAGAGCTGGCCAGGTGC
ERI1_siRNAres_HindII Rv	ACTCTCGGCATGGACGAGCTG
ERI1_siRNAres_KpnI FW	GTTAAACCCGCTGATCAGCCTCGA
M13 FW	GTAAAACGACGGCCAGT
M13 RV	CAGGAAACAGCTATGAC
ER1_Catalytic_dead_Fw	GTTATTATGACTACATTTGTATTATTGGCTTTGGAG CCACTTGTGAAGAAGG
ERI1_Catalytic_dead_Rv	CCTTCTTCACAAGTGGCTCCAAAGCCAATAATACAA ATGTAGTCATAATAAC

Table 3. List of primary antibodies

Protein	Host	Company	IF	WB
GFP	Mouse	Roche (11814460001)		1:1000
α-Tubulin	Mouse	Sigma (cloneDM1A, T6199)		1:5000
MRE11	Rabbit	Kind gift of Roland Kanaar		1:3000
ERI1	Rabbit	Cell signaling (405SS)		1:2000
p-RPA (S4/S8)	Rabbit	Bethyl Laboratories (A300-245A)	1:1000	1:1000
ETAA1	Rabbit	Kind gift of Niels Mailand		1:400
RPA	Mouse	Abcam (ab2175)	1:1000	1:1000

Supplementary Figures and Tables - Heading

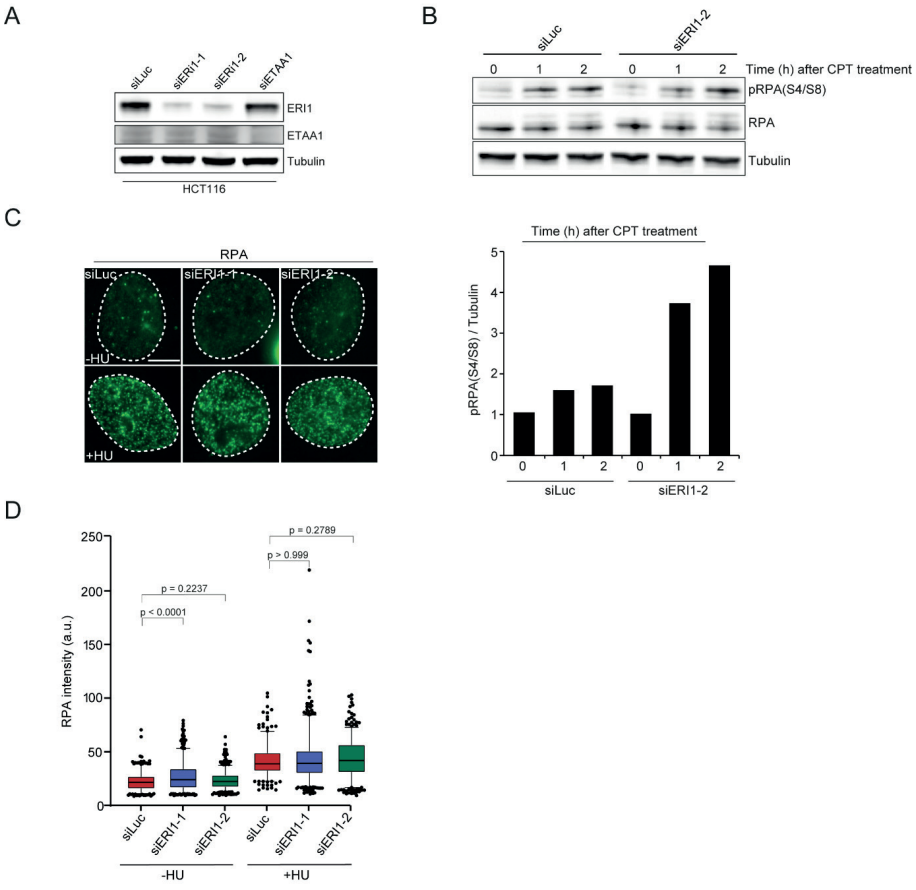

Supplementary Figure. 1 – related to Figure. 1. ERI1 protects cells against HU-induced RS. (A) Western blot analysis of ERI1 expression in cells from Figure 1B. Blots are probed for ERI1, ETAA1 and Tubulin. Tubulin is a loading control. (B) Western blot analysis of phosphorylated RPA32 (S4/S8) and RPA32 expression in cells transfected with the indicated siRNAs. Cells were examined after the indicated timepoint upon 1μM CPT treatment. Tubulin is a loading control (upper panel). Quantification of phosphorylated RPA32 (S4/S8) expression Tubulin is a loading control, which was used for normalization of phosphorylated RPA32 (S4/S8) expression. Data were normalized to siLuc UT, which was set to 1 (lower panel). (C) RPA foci formation in U2OS cells transfected with the indicated siRNAs. Cells were exposed to 2 mM of HU and foci intensity was measured after 4 hours. (D) Quantification of RPA intensity in cells from B. Mean foci intensity was quantified in immuno-stained RPA cells. The mean of 3 independent experiments is shown.

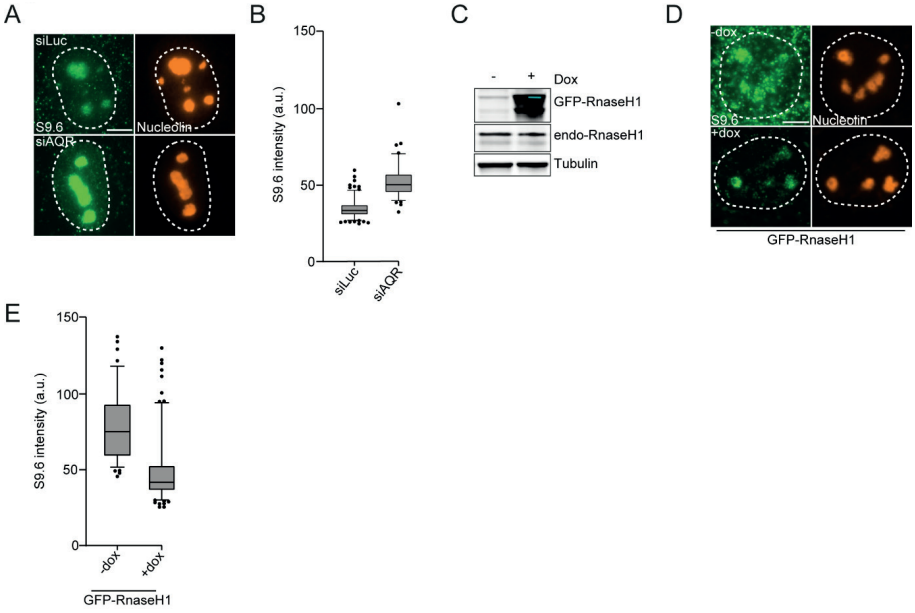

Supplementary Figure. 2 – related to Figure. 5. Validation of S9.6 staining. (A) S9.6 nuclear intensity was measured in U2OS cells transfected with the indicated siRNAs. The S9.6 signal intensity per nucleus was determined by subtracting the S9.6 staining with that from nucleoli in each nucleus. (B) Quantification of S9.6 intensity in cells from A. Mean intensity was quantified in immuno-stained S9.6 cells. *P*-values were derived from Kruskal–Wallis ANOVA Dunn's post test. (C) Expression levels of endogenous RnaseH1 and dox-inducible GFP-RnaseH1 in U2OS Flp-In/TRex cells. Tubulin is a loading control. (D) Effect of inducible expression of GFP-tagged RnaseH1 on S9.6 nuclear intensity U2OS Flp-In/TRex cells. The S9.6 signal intensity per nucleus was determined by subtracting the S9.6 staining with that from nucleoli in each nucleus. (E) Quantification of S9.6 intensity in cells from D. Mean intensity was quantified in immuno-stained S9.6 cells. *P*-values were derived from Kruskal–Wallis ANOVA Dunn's post test.

Supplementary Table 1

Supplementary Table 1. Statistical analysis comparing LFQ intensities of proteins identified by LC-MS/MS in GFP-pulldowns from U2OS Flp-In/T-Rex cells expressing either GFP-ERI1 or GFP-NLS in the presence and absence of HU
- Log p-value and average fold-enrichment (log2) are indicated. Additional information from the analysis of identified proteins is also included.

GENE			Eri1 Vs GFP			Eri1-HU Vs Eri1			Miscellaneus													Values								
Fasta headers	Protein names	Gene names	Significant (p<0.05)	-Log p-value	Difference (log2)	Significant (p<0.05)	-Log p-value	Difference (log2)	Peptides	Razor + unique peptides	Unique peptides	Sequence coverage [%]	Unique + razor sequence coverage [%]	Unique sequence coverage [%]	Mol. weight [kDa]	Q-value	Score	Intensity	MS/MS Count	Protein IDs	Majority protein IDs	ERI1-1	ERI1-2	ERI1-3	ERI1-HU-1	ERI1-HU-2	ERI1-HU-3	GFP-1	GFP-2	GFP-3
sp|P0425	Keratin, ty	KRT6B	+	3,18	-5,35		0,99	4,25	54	2	2	63,5	1,8	1,8	60,066	0	12,753	2606000000	5	P04259	P04259	20,90	22,71	22,01	22,64	26,35	29,36	26,88	27,33	27,46
sp|Q59GN	Putative 6	RPL39P5;RPL39		0,46	1,56		1,09	3,32	2	2	2	19,6	19,6	19,6	6,3225	0	13,751	739010000	13	Q59GN2;P	Q59GN2;P	22,05	25,92	21,33	26,41	26,73	26,12	21,62	22,07	20,92
sp|P68871	Hemoglob	HBB;HBD		0,80	-4,41		0,71	3,29	9	9	9	68	68	68	15,998	0	168,66	2919000000	59	P68871;F8	P68871;F8	21,16	20,39	22,71	22,19	28,68	23,27	23,27	30,76	23,46
sp|P11387	DNA topoi	TOP1		0,23	0,81		1,11	3,16	10	10	10	13,5	13,5	13,5	90,725	0	77,033	763240000	40	P11387;E5	P11387	20,96	25,17	24,68	27,05	26,55	26,67	23,54	22,24	22,60
sp|P47914	60S ribosa	RPL29		0,64	2,79		0,61	2,68	2	2	2	14,5	14,5	14,5	17,752	0	12,783	2067600000	17	P47914	P47914	21,41	27,47	27,09	28,35	27,80	27,87	22,21	22,81	22,60
tr|F5H6E2	Unconven	MYO1C		0,91	0,88		1,00	2,66	16	16	16	19,7	19,7	19,7	118,99	0	184,38	984910000	31	F5H6E2;O	F5H6E2;O	23,50	23,03	23,13	24,05	25,36	28,24	22,01	21,82	23,19
sp|Q96KR	Zinc finger	ZFR		0,00	0,00	+	3,02	2,47	3	3	3	4,1	4,1	4,1	117,01	0	25,73	130880000	5	Q96KR1;H	Q96KR1	21,21	21,85	21,55	24,41	23,93	23,68	22,54	23,34	21,40
tr|H0YD13	CD44 antig	CD44		0,65	-1,26	+	2,20	2,47	2	2	2	13,6	13,6	13,6	22,683	0	19,936	339650000	25	H0YD13;H	H0YD13;H	22,88	22,07	21,48	25,08	24,46	24,30	21,83	24,19	24,19
sp|P69905	Hemoglob	HBA1;HBA2		0,34	-2,46		0,56	2,33	7	7	4	62,7	62,7	40,1	15,257	0	119,38	1979200000	41	P69905;G	P69905;G	22,13	21,37	22,22	21,99	27,88	22,85	21,10	30,33	21,67
sp|Q9NZT	Calmoduli	CALML5		1,13	-3,43		0,52	2,28	13	13	13	91,1	91,1	91,1	15,892	0	323,31	4474900000	65	Q9NZT1	Q9NZT1	21,33	24,01	25,79	24,29	24,91	28,77	26,59	28,36	26,49
sp|P62081	40S ribosa	RPS7	+	2,74	2,23	+	3,75	2,05	7	7	7	47,9	47,9	47,9	22,127	0	147,34	4030400000	48	P62081;B5	P62081;B5	26,99	26,64	27,00	29,06	28,98	28,74	24,26	24,47	25,19
sp|Q9BVP	Guanine n	GNL3		0,00	0,00	+	1,69	1,97	3	3	3	5,6	5,6	5,6	60,54	0	19,425	174140000	5	Q9BVP2-2	Q9BVP2-2	22,85	21,14	22,54	24,24	24,19	24,02	21,66	22,68	23,17
tr|H0YLP6	60S ribosa	RPL28	+	2,95	3,80	+	1,93	1,78	4	4	4	37,1	37,1	37,1	9,657	0	33,555	3719400000	46	H0YLP6;H	H0YLP6;H	27,07	27,88	26,55	29,13	28,75	28,95	23,12	23,13	23,84
tr|A0A1B0GVI3|A0A1B0GVI3_HUMAN Kera				0,61	-1,54		0,66	1,74	7	5	5	47,7	32,7	32,7	10,03	0	33,406	548530000	21	A0A1B0GV	A0A1B0GV	22,19	21,84	23,69	22,28	25,82	24,86	23,90	25,89	22,55
sp|P84090	Enhancer	ERH		0,47	1,49		0,53	1,68	2	2	2	21,2	21,2	21,2	12,259	0	26,441	498870000	17	P84090;G	P84090;G	22,50	26,69	22,58	26,05	25,28	25,48	22,45	22,53	22,30
sp|P42766	60S ribosa	RPL35	+	1,65	3,74		1,07	1,64	5	5	5	32,5	32,5	32,5	14,551	0	36,147	1553400000	29	P42766;F2	P42766;F2	24,79	27,22	26,44	27,76	27,70	27,92	22,80	20,98	23,46
tr|E9PB61	THO comp	ALYREF		1,27	3,20	+	1,35	1,58	6	6	6	30,3	30,3	30,3	27,557	0	170,68	1709300000	55	E9PB61;Q	E9PB61;Q	26,95	26,29	25,08	27,78	27,57	27,71	21,86	25,00	21,84
sp|P62750	60S ribosa	RPL23A	+	2,78	4,40	+	1,58	1,57	10	10	10	48,7	48,7	48,7	17,695	0	89,657	5256600000	73	P62750;H	P62750;H	27,54	28,64	27,49	29,05	29,38	29,95	22,87	23,25	24,36
tr|C9JXB8	60S ribosa	RPL24	+	1,74	3,64	+	1,65	1,53	6	6	6	38	38	38	14,369	0	99,593	4039800000	79	C9JXB8;C9	C9JXB8;C9	26,97	28,19	26,95	29,11	28,77	28,82	24,13	22,09	24,96
sp|Q08211	ATP-depe	DHX9	+	2,74	2,29	+	3,10	1,43	30	30	30	28,9	28,9	28,9	140,96	0	323,31	6741700000	199	Q08211;Q	Q08211	27,97	28,43	28,09	29,71	29,62	29,46	25,33	26,25	26,05
sp|P62888	60S ribosa	RPL30	+	2,64	3,66	+	1,64	1,43	5	5	5	26,1	26,1	26,1	12,784	0	32,604	1696600000	22	P62888;E5	P62888;E5	25,99	26,56	25,92	27,41	27,10	28,26	21,90	22,11	23,47
tr|J3QLE5	Small nucl	SNRPN;SNRPB		0,77	2,05		0,57	1,42	3	3	3	17,8	17,8	17,8	17,546	0	18,379	309030000	23	J3QLE5;P	J3QLE5;P	24,48	24,80	21,40	25,23	24,75	25,05	21,69	20,56	22,38
sp|P18077	60S ribosa	RPL35A	+	2,78	3,71	+	1,30	1,39	6	6	6	46,4	46,4	46,4	12,538	0	48,245	2416400000	44	P18077;C9	P18077;C9	26,23	27,65	26,80	28,74	27,78	28,34	23,10	22,77	23,68
sp|Q1290	Interleukin	ILF3	+	2,80	4,59	+	2,03	1,38	20	20	20	33,6	33,6	33,6	95,337	0	323,31	4184300000	94	Q12906;Q	Q12906;Q	27,36	28,18	27,57	29,37	28,81	29,08	22,03	23,51	23,81
sp|O1547	Melanoma	MAGEB2	+	2,78	3,42	+	2,19	1,35	6	6	6	17,2	17,2	17,2	35,277	0	46,846	886040000	45	O15479;O	O15479	25,14	25,89	25,27	26,94	26,55	26,86	21,40	21,90	22,74
tr|A0A0A0	Ig gamma-	IGHG1;IGHG3;IGHG4		1,14	-2,34		0,40	1,35	4	4	3	12,3	12,3	10,5	43,911	0	67,362	488810000	24	A0A0A0M	A0A0A0M	21,35	22,05	24,43	22,25	25,97	23,66	25,33	25,06	24,47
sp|P39023	60S ribosa	RPL3	+	1,62	4,54	+	2,98	1,29	15	15	15	38,7	38,7	38,7	46,108	0	203,1	7965700000	136	P39023;G	P39023;G	28,42	28,89	28,58	30,00	29,79	29,95	24,62	21,67	25,98
tr|Q5JW30	Double-st	STAU1	+	2,16	3,07		0,92	1,28	10	10	10	22,1	22,1	22,1	54,708	0	121,43	1178500000	61	Q5JW30;Q	Q5JW30;Q	25,19	26,94	25,18	27,61	26,94	26,61	22,42	22,81	22,88
tr|F8W7C6	60S ribosa	RPL10	+	2,58	4,98	+	1,81	1,26	7	7	7	39,3	39,3	39,3	18,565	0	84,524	4385300000	83	F8W7C6;A	F8W7C6;A	27,46	28,25	27,42	28,93	28,73	29,25	22,48	21,68	24,04
sp|P40429	60S ribosa	RPL13A;RP	+	3,54	3,91	+	2,20	1,25	7	7	7	31,5	31,5	31,5	23,577	0	44,039	4480700000	58	P40429;Q	P40429;Q	27,75	28,15	27,65	29,46	28,84	29,00	24,13	23,37	24,34
sp|P62244	40S ribosa	RPS15A	+	2,36	2,97	+	2,16	1,25	5	5	5	45,4	45,4	45,4	14,839	0	77,045	3181600000	57	P62244;I3	P62244;I3	27,24	27,63	27,21	28,90	28,21	28,70	24,19	23,65	25,32
tr|F8W6I7	Heterogen	HNRNPA1	+	2,09	1,03	+	2,35	1,23	12	11	11	44,6	41,7	41,7	33,155	0	301,3	5557100000	157	F8W6I7;P	F8W6I7;P	27,63	28,17	27,69	29,28	28,84	29,07	26,59	27,00	26,82
sp|O7602	Ribosomal	RSL1D1	+	3,14	3,28	+	1,92	1,22	3	3	3	6,5	6,5	6,5	54,972	0	20,755	602490000	14	O76021;I3	O76021;I3	24,85	25,41	24,98	26,75	26,11	26,04	21,73	21,30	22,36
sp|P61254	60S ribosa	RPL26;RPL	+	3,04	4,65	+	1,63	1,22	7	7	7	37,9	37,9	37,9	17,258	0	67,927	3214800000	37	P61254;I3	P61254;I3	27,34	27,79	27,11	29,14	28,19	28,56	22,81	21,89	23,58
sp|P00167	Cytochrom	CYB5A		0,40	1,26		0,43	1,20	2	2	2	34,7	34,7	34,7	11,268	0	15,295	239670000	7	P00167-2;	P00167-2;	20,80	24,34	24,24	24,74	24,33	23,92	21,77	23,02	20,81
tr|D6RAN4	60S ribosa	RPL9	+	3,96	3,04	+	1,82	1,18	6	6	6	51,4	51,4	51,4	20,775	0	118,78	1374700000	50	D6RAN4;P	D6RAN4;P	25,96	26,12	26,12	26,69	27,46	27,60	22,85	22,83	23,42
tr|A0A0A0	U1 small n	SNRPC		0,80	1,78		0,51	1,18	2	2	2	11,7	11,7	11,7	19,687	0	12,748	240010000	3	A0A0A0M	A0A0A0M	24,21	24,41	21,31	24,63	24,53	24,31	22,00	21,21	21,36
sp|P07305	Histone H1	H1F0	+	2,24	3,15		1,27	1,18	7	7	7	27,8	27,8	27,8	20,863	0	52,924	1734800000	54	P07305;P	P07305;P	26,10	27,37	26,05	27,64	27,64	27,77	23,56	22,60	23,91
sp|P62899	60S ribosa	RPL31	+	2,56	4,08	+	1,67	1,17	7	7	7	41,6	41,6	41,6	14,463	0	71,83	6122600000	56	P62899;H	P62899;H	28,16	28,97	28,11	29,62	29,29	29,83	23,82	23,74	25,43
sp|Q9NR3	Nucleolar	DDX21	+	2,05	2,14	+	1,49	1,17	13	13	12	20,8	20,8	18,7	79,656	0	84,517	1447800000	49	Q9NR30-2	Q9NR30-2	26,36	26,57	25,59	27,70	27,00	27,32	24,24	23,38	24,49
tr|E5RHV7	Catenin al	CTNNA1		0,60	-1,64		0,84	1,15	2	2	2	26,8	26,8	26,8	13,448	0	19,879	8146500000	17	E5RHV7;E	E5RHV7;E	28,79	27,26	26,91	28,50	29,34	28,58	28,50	31,45	27,95
sp|P26373	60S ribosa	RPL13	+	1,73	4,03	+	1,88	1,14	10	10	10	43,6	43,6	43,6	24,261	0	182,23	11501000000	137	P26373;P2	P26373;P2	29,06	29,65	28,99	30,61	30,04	30,47	25,79	23,20	26,61
sp|P62917	60S ribosa	RPL8	+	2,41	4,10	+	1,86	1,14	6	6	6	22,2	22,2	22,2	28,024	0	86,839	6359600000	84	P62917;E9	P62917;E9	28,59	28,55	28,23	30,09	29,35	29,35	24,60	23,08	25,38
sp|O1537	Eukaryotic	EIF3D		0,27	-0,86		0,38	1,14	3	3	3	7	7	7	58,14	0	19,903	227910000	12	O15371-2;	O15371-2;	23,69	20,21	24,15	24,15	23,83	23,47	23,81	23,93	22,90
sp|Q02878	60S ribosa	RPL6	+	2,36	4,39	+	2,07	1,12	14	14	14	44,8	44,8	44,8	32,728	0	323,31	17956000000	163	Q02878;F	Q02878	29,84	30,33	29,80	31,40	30,86	31,06	25,89	24,20	26,69
sp|P62829	60S ribosa	RPL23	+	2,92	2,65	+	1,80	1,10	4	4	4	29,3	29,3	29,3	14,865	0	28,161	2122400000	29	P62829;C9	P62829;C9	26,74	27,50	26,82	28,38	28,00	27,98	24,40	23,98	24,72
sp|P61313	60S ribosa	RPL15	+	1,85	4,36	+	1,80	1,10	11	11	11	43,1	43,1	43,1	24,146	0	112,91	7328700000	103	P61313;E7	P61313;E7	28,50	29,10	28,33	29,96	29,48	29,79	24,41	22,46	25,99
sp|P18124	60S ribosa	RPL7	+	1,96	3,48	+	1,78	1,10	13	13	13	41,1	41,1	41,1	29,225	0	118,09	12074000000	124	P18124;A	P18124;A	29,17	29,70	29,20	30,74	30,03	30,59	25,85	24,57	27,20
tr|K7EJT5	60S ribosa	RPL22	+	1,49	3,02		1,11	1,09	2	2	2	51,1	51,1	51,1	5,0827	0	14,94	2460400000	29	K7EJT5;K7	K7EJT5;K7	26,58	27,80	26,82	28,65	27,73	28,08	22,34	24,72	25,07
tr|A0A087	60S ribosa	RPL17;RPL	+	2,13	3,76	+	1,72	1,08	6	6	6	39,6	39,6	39,6	19,586	0	136,33	6580600000	71	A0A087W	A0A087W	28,32	28,92	28,28	29,91	29,24	29,59	24,54	23,61	26,08
sp|P49207	60S ribosa	RPL34	+	3,85	4,64	+	1,78	1,07	4	4	4	21,4	21,4	21,4	13,293	0	28,088	2643400000	43	P49207	P49207	27,12	27,57	27,01	28,61	27,91	28,40	22,95	22,05	22,78
sp|P25398	40S ribosa	RPS12	+	3,36	3,17	+	1,90	1,07	3	3	3	30,3	30,3	30,3	14,515	0	187,79	5403900000	57	P25398	P25398	28,04	28,15	28,17	28,79	29,15	29,64	24,91	24,46	25,48
sp|P46778	60S ribosa	RPL21	+	2,83	5,17	+	1,66	1,07	7	7	7	41,2	41,2	41,2	18,565	0	113,29	4859700000	58	P46778;G	P46778	28,20	28,45	27,78	29,54	28,80	29,30	23,16	21,79	23,97
sp|Q1498	Nuclear m	NUMA1	+	2,46	2,43		1,30	1,06	14	14	14	8,3	8,3	8,3	236,51	0	112,48	488870000	43	Q14980-2;	Q14980-2;	24,60	25,09	24,62	26,51	25,63	25,36	22,10	23,05	21,87
sp|P36952	Serpin B5	SERPINB5		0,79	-1,79		0,27	1,06	3	3	3	11,5	11,5	11,5	42,1	0	30,427	219720000	9	P36952;P3	P36952;P3	22,12	19,97	23,07	20,96	25,17	22,20	24,00	24,02	22,51
sp|Q9Y3U	60S ribosa	RPL36	+	3,10	4,42	+	2,07	1,05	4	4	4	21	21	21	12,254	0	31,552	2325400000	50	Q9Y3U8;I	Q9Y3U8	26,95	27,45	26,98	28,46	28,04	28,01	23,12	21,79	23,19
sp|P62304	Small nucl	SNRPE	+	1,71	2,16	+	2,56	1,04	2	2	2	25	25	25	10,803	0	14,642	571780000	40	P62304;A	P62304;A	24,49	24,66	24,35	25,75	25,56	25,30	22,27	21,40	23,35
sp|P07476	Involucrin	IVL		1,06	-1,42		0,38	1,04	6	6	6	14,5	14,5	14,5	68,478	0	40,687	200440000	13	P07476	P07476	21,12	22,52	22,97	21,54	25,00	23,18	23,81	24,01	23,06
tr|F8W93	Insulin-like	IGF2BP2		0,50	0,58		0,96	1,03	4	4	4	9,8	9,8	9,8	66,785	0	25,981	104430000	6	F8W930;C	F8W930;C	22,67	23,47	21,97	24,22	23,39	23,58	22,14	22,58	21,65
tr|C9JQV0	Uncharact	C7orf50	+	3,63	4,04	+	1,83	1,03	3	3	3	28,6	28,6	28,6	21,883	0	44,822	747780000	26	C9JQV0;C	C9JQV0;C	25,09	25,84	25,44	26,63	26,23	26,59	21,07	21,88	21,33
sp|P62424	60S ribosa	RPL7A	+	2,46	4,32	+	1,56	1,02	11	11	11	33,1	33,1	33,1	29,995	0	99,607	9145200000	122	P62424;Q	P62424;Q	28,79	29,58	28,81	30,28	29,78	30,17	24,90	23,54	25,77
tr|J3KQN4	60S ribosa	RPL36A;RP	+	3,44	3,77	+	1,43	0,99	4	4	2	17,6	17,6	7	16,378	0	31,581	1367800000	42	J3KQN4;P	J3KQN4;P	26,11	26,83	26,23	27,69	26,93	27,52	22,51	22,26	23,10
tr|J3QR09	Ribosomal	RPL19	+	2,29	4,39	+	1,80	0,98	7	7	7	28	28	28	23,134	0	121,15	4034500000	71	J3QR09;J3	J3QR09;J3	27,67	28,34	27,84	29,12	28,67	29,02	23,20	22,46	25,03
tr|E9PJD9	60S ribosa	RPL27A	+	2,26	3,48	+	2,01	0,98	2	2	2	23,1	23,1	23,1	10,127	0	20,385	4421400000	40	E9PJD9;E9	E9PJD9;E9	27,84	28,34	27,96	29,33	28,83	28,93	24,73	23,42	25,55
tr|H7BXY3	Putative A	DHX30	+	3,49	5,12	+	1,42	0,97	21	21	21	23,1	23,1	23,1	130,55	0	192,91	1340900000	75	H7BXY3;Q	H7BXY3;Q	26,40	26,62	26,02	27,75	27,36	26,83	22,04	20,79	20,85
tr|M0R0F0	40S ribosa	RPS5	+	2,28	4,89		0,52	0,96	7	7	7	46,5	46,5	46,5	22,391	0	109,34	3321900000	59	M0R0F0;P	M0R0F0;P	26,28	28,57	27,71	29,08	27,58	28,78	22,72	21,58	23,59
sp|P62906	60S ribosa	RPL10A	+	3,49	4,91	+	1,81	0,96	8	8	8	31,3	31,3	31,3	24,831	0	66,468	3770000000	80	P62906	P62906	27,37	28,10	27,89	28,93	28,61	28,69	22,84	22,25	23,52
tr|D6RF44	Heterogen	HNRNPD		1,19	2,06		0,63	0,96	3	2	2	30,6	23,4	23,4	12,553	0	15,752	467310000	18	D6RF44;H	D6RF44;H	24,52	22,60	24,65	24,53	25,03	25,09	22,00	22,59	20,98
tr|X6RGJ2	Heterochr	HP1BP3	+	1,97	2,41		1,17	0,95	7	7	7	25,4	25,4	25,4	36,514	0	55,225	659240000	46	X6RGJ2;Q	X6RGJ2;Q	24,98	25,98	24,75	26,28	26,13	26,15	22,30	23,56	22,61
tr|E7EPB3	60S ribosa	RPL14	+	2,97	4,34	+	1,76	0,94	2	2	2	19,4	19,4	19,4	14,558	0	27,534	3568000000	52	E7EPB3;P	E7EPB3;P	27,70	28,18	27,53	28,99	28,51	28,74	23,55	22,60	24,24
sp|Q0706	Cytoskelet	CKAP4		0,51	-1,15		0,41	0,94	7	7	7	15	15	15	66,022	0	44,601	377690000	11	Q07065	Q07065	24,45	24,40	21,54	24,39	24,73	24,10	24,29	25,09	24,48
sp|Q8IY81	pre-rRNA (	FTSJ3	+	1,97	1,08		1,24	0,94	3	3	3	4,6	4,6	4,6	96,557	0	24,485	134220000	9	Q8IY81	Q8IY81	22,79	23,22	23,18	24,63	23,52	23,86	22,37	21,79	21,79
sp|P36578	60S ribosa	RPL4	+	2,19	3,53	+	1,73	0,94	12	12	12	31,9	31,9	31,9	47,697	0	121,14	17471000000	142	P36578;H	P36578;H	29,76	30,45	29,79	31,12	30,80	30,90	26,45	25,36	27,58
sp|P42357	Histidine a	HAL	+	1,67	-1,97		0,56	0,94	5	5	5	9,7	9,7	9,7	72,697	0	32,426	216450000	10	P42357;P4	P42357;P4	21,89	23,12	21,38	23,63	23,59	21,99	23,87	24,36	24,07
tr|E9PDF6	Unconven	MYO1B		0,72	1,01		0,56	0,93	7	7	7	7,5	7,5	7,5	128,48	0	52,793	216650000	10	E9PDF6;O	E9PDF6;O	23,13	22,85	22,70	23,10	23,10	25,29	22,63	20,64	22,40
sp|P08579	U2 small n	SNRPB2		1,21	0,98		0,83	0,92	4	4	4	20,9	20,9	20,9	25,486	0	34,628	307660000	17	P08579;M	P08579	23,58	24,66	23,48	25,53	24,43	24,53	23,01	22,83	22,94
sp|O6050	Heterogen	SYNCRIP	+	2,90	2,70	+	1,81	0,92	20	14	14	40,1	32,6	32,6	69,602	0	229,17	3022100000	90	O60506;O	O60506;O	27,18	27,79	27,42	28,21	28,66	28,26	25,32	24,55	24,41
sp|Q8NC5	Plasminog	SERBP1		0,10	0,23		0,66	0,91	3	3	3	13,2	13,2	13,2	42,426	0	57,127	340610000	23	Q8NC51-4	Q8NC51-4	24,28	24,47	22,68	24,77	25,17	24,23	22,40	23,88	24,45
sp|P62913	60S ribosa	RPL11	+	3,78	1,38	+	2,26	0,91	5	5	5	36,5	36,5	36,5	20,252	0	65,483	3792400000	68	P62913;P6	P62913;P6	27,74	27,72	27,50	28,83	28,32	28,53	26,28	26,15	26,38
tr|H3BLZ8	Probable (	DDX17		0,94	2,42		0,35	0,90	8	4	4	12,2	6,2	6,2	80,439	0	25,414	744980000	6	H3BLZ8;Q	H3BLZ8;Q	22,35	25,35	25,52	25,44	25,66	24,83	21,15	23,21	21,58
sp|P47929	Galectin-7	LGALS7	+	1,52	-1,82		0,38	0,89	7	7	7	62,5	62,5	62,5	15,075	0	72,328	4202900000	95	P47929	P47929	25,48	26,11	27,07	25,52	28,53	27,30	28,06	28,55	27,51
tr|B4DY09	Interleukin	ILF2	+	3,16	2,53	+	1,57	0,89	6	6	6	23	23	23	38,91	0	55,551	2157300000	59	B4DY09;Q	B4DY09;Q	26,93	27,56	26,71	28,08	27,85	27,95	24,36	24,61	24,63
tr|A0A0C4	Dolichyl-d	DDOST	+	3,33	-2,82		0,38	0,89	4	4	4	13,7	13,7	13,7	48,799	0	68,128	600120000	13	A0A0C4DG	A0A0C4DG	22,31	22,04	22,49	21,53	23,05	24,93	25,26	25,40	24,64
tr|D6RG13	40S ribosa	RPS3A	+	3,48	5,17		1,22	0,89	11	11	11	43,9	43,9	43,9	25,608	0	119,37	11343000000	135	D6RG13;P	D6RG13;P	29,42	29,78	29,05	30,77	29,84	30,31	23,62	24,15	24,99
tr|K7EM5	40S ribosa	RPS15	+	3,48	5,69		1,17	0,89	6	6	6	53,6	53,6	53,6	12,99	0	144,95	4647400000	68	K7EM56;A	K7EM56;A	27,85	28,55	28,15	28,72	28,83	29,65	22,46	21,73	23,30
sp|P61353	60S ribosa	RPL27	+	2,01	3,94	+	1,61	0,88	6	6	6	48,5	48,5	48,5	15,798	0	167,06	7138400000	76	P61353;K7	P61353;K7	28,80	29,16	28,43	29,93	29,46	29,64	24,54	23,61	26,42
sp|P05388	60S acidic	RPLP0;RPL	+	2,36	2,90	+	1,93	0,88	8	8	8	34,7	34,7	34,7	34,273	0	141,41	7389200000	116	P05388;F8	P05388;F8	28,51	29,06	28,66	29,50	29,52	29,86	26,25	24,91	26,38
sp|Q9NUC	SPATS2-lik	SPATS2L	+	2,81	2,02		0,99	0,88	4	4	4	11,5	11,5	11,5	54,178	0	28,818	188180000	8	Q9NUQ6-2	Q9NUQ6-2	23,74	23,93	23,22	25,13	23,89	24,50	21,73	21,30	21,81
sp|Q9UM	Pre-mRNA	PRPF19	+	1,62	1,50		0,90	0,84	8	8	8	21,8	21,8	21,8	55,18	0	59,203	1208800000	47	Q9UMS4;F	Q9UMS4;F	25,67	26,85	25,59	27,08	26,59	26,96	24,35	24,74	24,52
tr|D6R9P3	Heterogen	HNRNPAB	+	2,78	2,62	+	1,74	0,84	5	5	5	19,6	19,6	19,6	30,302	0	54,6	1170800000	41	D6R9P3;D	D6R9P3;D	25,89	26,59	26,14	27,17	26,95	27,00	23,37	24,14	23,23
sp|P62851	40S ribosa	RPS25	+	2,68	3,25	+	1,30	0,83	7	7	7	36	36	36	13,742	0	85,541	9836000000	73	P62851;E9	P62851	29,14	29,69	28,93	30,48	29,91	29,87	25,97	25,32	26,71
sp|P05387	60S acidic	RPLP2	+	2,79	2,43	+	1,45	0,83	7	7	7	77,4	77,4	77,4	11,665	0	293,75	13502000000	152	P05387;H	P05387	29,42	30,15	29,42	30,71	30,37	30,40	27,22	26,88	27,61
sp|P25311	Zinc-alpha	AZGP1	+	3,32	-2,09		0,98	0,83	3	3	3	14,4	14,4	14,4	34,258	0	17,89	218500000	11	P25311;C9	P25311	22,42	22,16	22,16	22,60	22,79	23,84	24,10	24,21	24,69
sp|Q0083	Heterogen	HNRNPU	+	3,02	1,91	+	1,40	0,80	23	23	2	28,6	28,6	2,4	90,583	0	323,31	25627000000	380	Q00839;Q	Q00839	30,29	30,91	30,25	31,60	31,10	31,15	28,57	28,66	28,50
sp|P09382	Galectin-1	LGALS1		0,59	-1,62		0,25	0,79	4	4	4	31,1	31,1	31,1	14,716	0	27,466	1363200000	24	P09382	P09382	26,34	22,54	26,12	25,87	25,86	25,63	26,65	26,50	26,72
tr|H0Y7A7	Calmoduli	CALM2;CALM1;CALM		0,25	0,30		0,69	0,78	8	8	6	46	46	42,2	20,762	0	106,24	1726700000	46	H0Y7A7;P	H0Y7A7;P	25,86	25,87	25,68	26,14	26,01	27,61	24,72	26,34	25,45
sp|P62753	40S ribosa	RPS6	+	1,57	4,69	+	1,63	0,78	8	8	8	24,5	24,5	24,5	28,68	0	167,79	11585000000	102	P62753;A	P62753;A	29,23	29,82	29,31	30,44	30,03	30,24	25,86	22,06	26,38
sp|Q6UW	Suprabasin	SBSN	+	2,56	-1,40		0,59	0,77	9	9	9	34,9	34,9	34,9	60,54	0	236,58	1161300000	92	Q6UWP8;	Q6UWP8	25,04	24,75	25,20	24,84	25,66	26,81	26,56	26,58	26,06
tr|J3QQ67	60S ribosa	RPL18	+	2,08	4,83		0,97	0,77	7	7	7	36,3	36,3	36,3	21,728	0	90,768	7208700000	41	J3QQ67;Q	J3QQ67;Q	28,48	29,39	28,96	30,15	29,75	29,24	24,85	22,22	25,28
tr|I3L1L3|	Myb-bindi	MYBBP1A	+	2,54	1,94	+	1,63	0,77	5	5	5	4,5	4,5	4,5	140,13	0	32,808	186610000	28	I3L1L3;Q9	I3L1L3;Q9	23,52	23,62	23,04	24,39	24,13	23,98	21,15	21,93	21,30
sp|Q8WV	Protein PO	POF1B	+	1,79	-1,73		0,39	0,76	8	8	8	16,5	16,5	16,5	68,064	0	72,558	1325300000	87	Q8WVV4;	Q8WVV4;	24,44	24,58	25,56	24,20	26,03	26,61	26,68	26,96	26,11
tr|A0A0J9	Ras GTPas	IQGAP1		0,18	-0,44		0,54	0,75	6	6	5	6,2	6,2	5,5	136	0	47,159	193240000	20	A0A0J9YX	A0A0J9YX	23,27	23,24	21,51	23,31	23,81	23,15	21,72	23,95	23,67
sp|Q969Q	60S ribosa	RPL36AL	+	2,93	0,94		1,28	0,75	4	2	2	23,6	9,4	9,4	12,469	0	12,585	101570000	7	Q969Q0	Q969Q0	22,48	22,72	22,55	23,09	23,86	23,05	21,48	21,78	21,68
sp|P27482	Calmoduli	CALML3		0,14	-0,67		0,23	0,74	8	6	6	69,8	59,7	59,7	16,891	0	82,221	569160000	20	P27482	P27482	21,30	21,96	24,82	24,52	23,64	22,15	22,25	26,18	21,66
tr|M0QZC	40S ribosa	RPS11	+	3,88	3,01	+	1,45	0,73	6	6	6	41,5	41,5	41,5	13,997	0	38,798	7851100000	91	M0QZC5;P	M0QZC5;P	28,90	29,20	28,68	29,93	29,32	29,72	25,77	25,77	26,20
sp|Q1315	Heterogen	HNRNPA0	+	2,05	1,03	+	2,25	0,72	6	6	6	28,5	28,5	28,5	30,84	0	70,494	2184800000	83	Q13151	Q13151	26,54	26,90	26,92	27,47	27,45	27,61	25,44	25,78	26,05
tr|G3V4W	Heterogen	HNRNPC	+	3,12	2,06	+	1,43	0,72	16	16	1	51,9	51,9	6,9	28,916	0	234,96	10837000000	247	G3V4W0;E	G3V4W0;	29,20	29,72	29,15	30,35	29,84	30,03	27,50	27,06	27,33
tr|A0A024	40S ribosa	RPS9	+	2,74	3,81	+	1,41	0,72	15	15	15	53,1	53,1	53,1	22,591	0	109,5	22353000000	185	A0A024R4	A0A024R4	30,41	30,92	30,25	31,48	31,05	31,20	26,88	25,82	27,46
sp|Q5JTH	RRP12-like	RRP12	+	3,77	5,23		0,96	0,71	15	15	15	15,2	15,2	15,2	132,71	0	134,65	1362800000	92	Q5JTH9-2;	Q5JTH9-2;	26,30	27,26	26,23	27,50	27,15	27,28	21,66	21,45	21,01
sp|P60866	40S ribosa	RPS20	+	4,36	4,24	+	1,38	0,71	3	3	3	22,7	22,7	22,7	13,373	0	30,803	5096300000	62	P60866;P6	P60866;P6	28,49	28,83	28,27	29,53	28,92	29,27	24,26	24,06	24,57
sp|P62266	40S ribosa	RPS23	+	2,14	3,12	+	1,44	0,70	6	6	6	30,1	30,1	30,1	15,807	0	44,377	5440400000	76	P62266;D	P62266;D	28,22	28,82	28,14	29,20	28,95	29,13	25,39	24,22	26,21
sp|P08708	40S ribosa	RPS17	+	3,36	4,12		1,00	0,69	5	5	5	47,4	47,4	47,4	15,55	0	323,31	3934400000	67	P08708;H	P08708;H	27,63	27,83	28,11	28,06	29,07	28,51	23,84	23,07	24,30
sp|P30050	60S ribosa	RPL12	+	2,62	3,24	+	1,65	0,69	3	3	3	23,6	23,6	23,6	17,818	0	74,809	2663100000	55	P30050;P3	P30050	27,14	27,79	27,38	28,12	28,19	28,08	24,33	23,39	24,89
sp|P09874	Poly [ADP-	PARP1	+	2,57	5,74		0,73	0,69	26	26	26	29,7	29,7	29,7	113,08	0	222,23	4889900000	181	P09874	P09874	27,86	29,18	28,31	29,50	29,05	28,87	22,62	21,43	24,10
tr|A0A0A6	E3 ubiquit	ZFP91-CNTF;ZFP91		0,74	0,37		0,96	0,68	2	2	2	7	7	7	59,57	0	14,481	73225000	5	A0A0A6YY	A0A0A6YY	22,23	22,64	22,16	23,61	22,68	22,77	21,73	21,86	22,32
sp|P62277	40S ribosa	RPS13	+	3,23	3,00	+	1,56	0,67	7	7	7	43	43	43	17,222	0	80,983	10813000000	156	P62277;I3	P62277;I3	29,31	29,84	29,29	30,26	29,99	30,19	26,70	25,99	26,75
sp|Q9Y2X	Nucleolar	NOP58		0,74	1,51		0,31	0,65	2	2	2	5,1	5,1	5,1	59,578	0	16,436	121590000	5	Q9Y2X3	Q9Y2X3	23,64	23,45	21,02	23,67	23,25	23,14	21,37	21,79	20,40
sp|P48594	Serpin B4	SERPINB4	+	2,61	-2,03		0,22	0,65	17	17	7	55,9	55,9	27,4	44,853	0	198,61	3152500000	150	P48594;H	P48594;H	25,05	25,70	26,03	25,20	28,46	25,07	27,73	27,66	27,47
sp|Q1383	Plakophilin	PKP1	+	1,51	-1,39		0,28	0,65	14	14	14	21,8	21,8	21,8	80,496	0	106,55	2106600000	95	Q13835-2;	Q13835-2;	25,33	25,24	26,41	24,93	26,10	27,90	27,44	26,96	26,77
tr|J3QRS3	Myosin re	MYL12A;MYL12B;MY		0,77	-0,42		0,57	0,65	4	4	4	32,2	32,2	32,2	20,457	0	55,297	669210000	16	J3QRS3;P1	J3QRS3;P1	24,70	24,28	25,03	24,44	25,55	25,96	25,25	25,18	24,85
sp|P62701	40S ribosa	RPS4X;RPS	+	3,69	2,71	+	1,58	0,64	11	11	11	37,3	37,3	37,3	29,597	0	84,826	11462000000	114	P62701;C9	P62701;C9	29,47	29,79	29,36	30,45	30,00	30,10	26,73	26,62	27,16
sp|A0A0C4DH42|HV3		IGHV3-66		0,52	-1,69		0,30	0,62	2	1	1	25,9	19,8	19,8	12,698	0	18,031	625440000	22	A0A0C4DH	A0A0C4DH	23,92	21,99	24,19	23,09	24,73	24,14	26,51	26,11	22,56
sp|P51991	Heterogen	HNRNPA3	+	3,13	1,20	+	2,25	0,62	8	8	8	30,2	30,2	30,2	39,594	0	163,5	4378400000	151	P51991;P5	P51991;P5	27,85	28,10	27,79	28,65	28,53	28,43	26,56	26,72	26,87
sp|Q9H0U	Ras-relate	RAB1B		0,36	1,30		0,22	0,62	9	3	3	57,7	22,9	22,9	22,171	0	20,263	275450000	13	Q9H0U4;E	Q9H0U4;E	24,37	24,88	21,40	24,51	24,11	23,90	20,76	24,24	21,75
tr|Q5JR95	40S ribosa	RPS8	+	2,90	3,89	+	1,52	0,61	7	7	7	42	42	42	21,879	0	201,24	20068000000	116	Q5JR95;P6	Q5JR95;P6	30,38	30,81	30,27	31,24	30,93	31,12	26,59	25,81	27,38
sp|O4339	Heterogen	HNRNPR	+	3,83	3,12		1,28	0,61	24	24	18	40,8	40,8	33,3	70,942	0	323,31	9516800000	183	O43390;O	O43390;O	29,17	29,82	29,32	30,26	29,96	29,92	26,52	26,26	26,19
sp|P62854	40S ribosa	RPS26;RPS	+	3,57	1,44	+	1,64	0,61	4	4	4	40	40	40	13,015	0	36,37	5228200000	88	P62854;Q	P62854;Q	28,31	28,54	28,23	29,24	28,76	28,90	27,05	26,80	26,91
sp|Q9UNC	Probable c	DIMT1	+	1,97	2,23		0,68	0,60	5	5	5	18,2	18,2	18,2	35,236	0	37,976	279660000	12	Q9UNQ2;A	Q9UNQ2;A	23,92	25,01	24,06	25,36	24,71	24,72	22,15	21,46	22,69
sp|P23396	40S ribosa	RPS3	+	3,09	3,34		1,29	0,59	13	13	13	59,3	59,3	59,3	26,688	0	213,49	20981000000	214	P23396;E9	P23396;E9	30,36	30,75	30,11	31,20	30,85	30,95	27,21	26,46	27,52
sp|O7553	Barrier-to-	BANF1	+	2,36	3,55		0,65	0,59	4	4	4	50,6	50,6	50,6	10,058	0	70,555	733020000	24	O75531	O75531	25,15	26,16	25,37	25,76	26,02	26,68	21,83	21,20	22,99
sp|P62249	40S ribosa	RPS16;ZNF	+	4,28	4,94		1,14	0,59	8	8	8	49,3	49,3	49,3	16,445	0	68,815	10012000000	103	P62249;M	P62249;M	29,44	29,97	29,48	30,56	29,98	30,13	24,77	24,29	25,00
sp|P15880	40S ribosa	RPS2	+	4,01	3,46	+	1,34	0,59	9	9	9	36,2	36,2	36,2	31,324	0	163,9	15639000000	104	P15880;E9	P15880;E9	29,87	30,28	29,90	30,75	30,29	30,78	26,65	26,21	26,81
sp|P39019	40S ribosa	RPS19	+	3,16	3,45		1,23	0,59	12	12	12	51,7	51,7	51,7	16,06	0	91,751	5913900000	121	P39019;A	P39019;A	28,52	29,07	28,51	29,53	29,21	29,12	25,30	24,68	25,76
tr|A0A140	Flotillin-1	FLOT1		0,38	-0,59		0,33	0,57	3	3	3	10,6	10,6	10,6	39,777	0	29,529	142340000	12	A0A140T9	A0A140T9	23,13	23,30	21,38	23,09	23,85	22,58	22,75	23,54	23,28
sp|Q0253	Histone H1	HIST1H1A	+	2,37	3,13	+	1,68	0,57	8	5	5	39,1	29,3	29,3	21,842	0	59,916	1124300000	56	Q02539	Q02539	26,30	26,47	26,33	27,16	26,97	26,67	23,59	22,18	23,93
sp|P15924	Desmoplak	DSP	+	2,13	-1,41		0,30	0,55	119	119	119	38,8	38,8	38,8	331,77	0	323,31	46414000000	1392	P15924;P1	P15924;P1	30,11	29,97	30,75	29,72	30,61	32,16	31,95	31,65	31,45
sp|P22087	rRNA 2-O-	FBL		0,48	0,32		0,75	0,55	4	4	4	26,5	26,5	26,5	33,784	0	33,616	284910000	8	P22087;M	P22087;M	24,12	24,26	23,88	24,19	24,47	25,25	23,84	23,27	24,18
tr|Q49AN	Small nucl	SNRPG;SN	+	2,86	2,91	+	1,66	0,54	2	2	2	29,7	29,7	29,7	7,1013	0	13,479	343040000	9	Q49AN9;F	Q49AN9;F	24,48	24,63	24,57	24,83	25,14	25,31	22,19	21,80	20,96
sp|P62879	Guanine n	GNB2;GNB1;GNB4		0,93	0,36		0,48	0,54	5	5	5	13,5	13,5	13,5	37,331	0	32,139	405340000	17	P62879;C9	P62879;C9	24,30	24,45	23,84	24,76	23,95	25,49	23,85	23,81	23,84
tr|E7EPN9	Protein PR	PRRC2C		0,36	1,29		0,60	0,53	9	9	9	3,4	3,4	3,4	308,77	0	52,485	1538500000	23	E7EPN9;Q	E7EPN9;Q	26,18	26,94	26,28	27,55	26,47	26,97	26,74	22,21	26,56
tr|A0A1B0	Cathepsin	CTSD	+	2,74	-2,64		0,27	0,53	6	6	6	17	17	17	43,688	0	49,758	352110000	17	A0A1B0GV	A0A1B0GV	22,97	21,99	22,21	21,84	22,63	24,28	25,44	24,89	24,76
sp|P62269	40S ribosa	RPS18	+	3,42	4,21		0,89	0,52	9	9	9	48,7	48,7	48,7	17,718	0	72,673	15981000000	104	P62269;I3	P62269	30,04	30,58	29,88	31,00	30,42	30,63	25,74	25,54	26,57
sp|Q9971	3-hydroxy	HSD17B10		0,64	-1,05		0,29	0,51	4	4	4	28,6	28,6	28,6	25,984	0	28,276	398200000	14	Q99714-2;	Q99714-2;	24,65	24,49	22,47	24,48	24,44	24,23	25,03	25,26	24,48
sp|P46087	Probable (	NOP2		1,02	1,34		1,25	0,51	9	9	9	14,6	14,6	14,6	88,972	0	69,642	715330000	44	P46087-2;	P46087-2;	25,55	26,00	25,44	26,21	26,29	26,00	24,94	23,13	24,89
tr|F8W1R7	Myosin lig	MYL6		0,48	0,20	+	1,45	0,49	5	5	5	34,5	34,5	34,5	16,29	0	36,739	709580000	44	F8W1R7;J	F8W1R7;J	25,30	25,01	25,09	25,43	25,57	25,88	24,71	25,24	24,84
sp|Q1661	Extracellul	ECM1		0,26	-0,78		0,19	0,49	2	2	2	6,5	6,5	6,5	46,099	0	13,408	148380000	15	Q16610-2;	Q16610-2;	22,90	20,30	22,20	23,04	22,79	21,03	24,34	21,68	21,70
sp|O7609	Signal reco	SRP72	+	3,27	2,30		0,88	0,49	16	16	16	30	30	30	74,605	0	194,37	2919500000	85	O76094;O	O76094;O	27,58	28,03	27,32	28,43	27,96	28,00	25,26	25,25	25,53
sp|P22626	Heterogen	HNRNPA2	+	2,71	0,56	+	1,78	0,48	14	14	13	45,6	45,6	43,1	37,429	0	196,76	6057600000	213	P22626;P2	P22626;P2	28,33	28,53	28,29	29,05	28,84	28,72	27,77	27,85	27,84
tr|Q5QPL	RNA-bindi	RALY	+	3,74	3,91	+	1,30	0,48	11	11	11	48,1	48,1	48,1	24,665	0	74,541	2345400000	52	Q5QPL9;Q	Q5QPL9;Q	27,35	27,84	27,41	27,98	27,90	28,17	23,95	23,13	23,78
sp|P62857	40S ribosa	RPS28	+	3,48	5,59		0,64	0,46	2	2	2	30,4	30,4	30,4	7,8409	0	17,883	3294900000	27	P62857	P62857	27,76	28,50	27,75	28,84	28,16	28,38	22,48	21,66	23,11
sp|P05109	Protein S1	S100A8	+	1,72	-1,54		0,27	0,46	6	6	6	40,9	40,9	40,9	10,834	0	41,06	2570700000	67	P05109	P05109	25,72	25,83	25,88	25,60	27,62	25,59	26,87	28,16	27,04

sp|P3557	Myosin-9	MYH9		0,88	-0,33		0,74	0,45	31	31	28	20,2	20,2	18,2	226,53	0	323,31	4434600000	262	P35579;P3	P35579;P3	27,68	27,30	27,60	27,49	28,08	28,35	27,76	28,11	27,69
sp|P6226	40S ribosa	RPS14	+	3,08	2,82		0,69	0,42	7	7	7	39,1	39,1	39,1	16,273	0	84,72	9089600000	91	P62263;HC	P62263;HC	29,15	29,65	28,79	29,86	29,55	29,44	26,64	26,02	26,48
sp|P0670	Protein S1	S100A9	+	1,44	-1,82		0,20	0,40	10	10	10	74,6	74,6	74,6	13,242	0	297,21	11566000000	181	P06702	P06702	27,55	27,56	28,38	27,51	29,64	27,53	29,08	30,69	29,18
sp|Q9UHE	Signal rec	SRP68	+	3,14	1,71		0,62	0,40	15	15	15	25,7	25,7	25,7	70,729	0	128,92	1641500000	98	Q9UHB9;C	Q9UHB9;C	26,66	27,18	26,62	27,66	27,06	26,93	25,07	25,13	25,12
sp|P4677	60S ribosa	RPL5	+	2,45	3,73		0,22	0,39	7	7	7	25,6	25,6	25,6	34,362	0	55,455	2510000000	64	P46777;Q	P46777	26,62	28,29	27,61	28,48	26,94	28,26	23,98	23,07	24,28
tr|Q5SRN	HLA class I	HLA-A;HLA-C;HLA-H		0,49	-0,77		0,21	0,38	3	2	1	15,1	10,7	2,7	34,211	0	26,429	325010000	13	Q5SRN7;A	Q5SRN7;A	24,22	24,41	22,27	24,27	24,07	23,70	24,43	24,38	24,40
tr|M0R3D	60S ribosa	RPL18A	+	3,40	3,51		0,38	0,38	6	6	6	35,5	35,5	35,5	16,714	0	36,721	2146500000	27	M0R3D6;N	M0R3D6;N	27,08	27,40	27,32	28,43	27,11	27,39	23,90	23,16	24,20
sp|P5413	Arginine-t	RARS		0,39	-0,41		0,37	0,38	2	2	2	3	3	3	75,378	0	12,681	177330000	6	P54136;E5	P54136;E5	23,51	23,62	22,32	23,39	23,65	23,55	23,56	23,82	23,30
sp|P08621	U1 small n	SNRNP70		1,15	2,34		1,20	0,36	8	8	8	17,3	17,3	17,3	50,617	0	53,932	663130000	19	P08621-2;	P08621-2;	25,31	25,48	25,37	25,96	25,77	25,51	22,45	24,91	21,77
tr|F8W7S	Ribosome-	RRBP1		0,55	0,32		0,69	0,35	3	3	3	4,4	4,4	4,4	84,325	0	18,717	122460000	6	F8W7S5;A	F8W7S5;A	22,61	22,82	22,79	23,46	23,12	22,69	22,74	21,94	22,58
sp|Q9H6F	Coiled-coil	CCDC86	+	2,10	2,09		1,06	0,35	2	2	2	16,3	16,3	16,3	12,743	0	11,585	213870000	6	Q9H6F5-2,	Q9H6F5-2,	24,22	24,38	23,87	24,47	24,58	24,47	22,07	21,37	22,75
tr|H7C3I1	Putative p	ST13;ST13P4;ST13P5		0,26	-0,58		0,14	0,34	3	3	3	25,3	25,3	25,3	16,219	0	19,483	209490000	22	H7C3I1;F6	H7C3I1;F6	24,10	21,48	24,01	23,98	23,29	23,33	23,48	24,26	23,60
sp|P1640	Histone H1	HIST1H1C;	+	2,82	2,38		0,46	0,33	10	10	3	36,6	36,6	12,2	21,364	0	73,226	13297000000	123	P16403;P1	P16403;P1	29,95	30,29	29,56	30,72	30,03	30,05	27,66	27,13	27,88
sp|Q1677	Histone H2	HIST2H2A	+	2,31	2,59		0,40	0,33	6	6	1	60,5	60,5	22,5	13,988	0	171,49	82491000000	125	Q16777;Q	Q16777;Q	32,96	32,13	32,76	33,43	32,66	32,75	30,02	29,35	30,69
sp|Q1514	Plectin	PLEC		0,81	-0,42		0,72	0,32	60	60	57	16,6	16,6	15,5	512,6	0	323,31	4873500000	273	Q15149-7;	Q15149-7;	27,63	27,88	27,95	28,28	28,35	27,78	28,24	27,86	28,63
sp|P35251	Replicatio	RFC1	+	2,40	0,85		0,66	0,32	3	3	3	3	3	3	128,18	0	20,625	149140000	21	P35251-2;	P35251-2;	23,15	23,31	23,61	24,01	23,46	23,55	22,42	22,57	22,52
sp|Q96H7	Zinc finger	ZC3HAV1L		0,21	-0,53		0,11	0,31	3	3	3	14	14	14	32,962	0	31,774	365220000	25	Q96H79;Q	Q96H79	25,41	24,77	22,26	25,18	24,35	23,85	24,75	24,74	24,55
tr|B4DXZ6	Fragile X m	FXR1		0,92	0,34		0,82	0,31	4	4	4	11,7	11,7	11,7	68,326	0	48,399	504990000	19	B4DXZ6;P5	B4DXZ6;P5	24,78	25,01	24,54	24,95	25,30	25,00	24,62	24,25	24,43
sp|Q0241	Desmoglei	DSG1	+	1,81	-1,23		0,16	0,31	21	21	21	27,9	27,9	27,9	113,75	0	323,31	11589000000	324	Q02413;Q	Q02413	28,34	28,06	28,95	27,97	28,22	30,08	29,94	29,70	29,41
sp|Q1415	Eukaryotic	EIF3A		0,22	0,56		0,14	0,31	5	5	5	5	5	5	162,63	0	29,007	111530000	5	Q14152-2;	Q14152-2,	21,48	24,21	23,22	22,99	23,69	23,15	23,39	21,30	22,55
sp|P1492	Junction p	JUP	+	2,24	-1,39		0,16	0,30	24	24	24	37,9	37,9	37,9	81,744	0	323,31	15863000000	478	P14923;C9	P14923	28,56	28,71	29,23	28,10	28,92	30,37	30,53	30,13	30,00
tr|E9PEB5	Far upstre	FUBP1		0,64	-0,83		0,27	0,30	5	5	5	8,7	8,7	8,7	68,903	0	30,795	379630000	24	E9PEB5;Q	E9PEB5;Q	24,46	22,97	23,77	24,13	23,83	24,14	23,79	25,12	24,79
sp|P63261	Actin, cyto	ACTG1;AC	+	2,10	-0,66		0,68	0,30	18	18	6	52	52	24,8	41,792	0	323,31	44061000000	572	P63261;P6	P63261;P6	30,84	30,48	30,80	30,68	31,10	31,23	31,45	31,44	31,22
tr|A0A087	Heterogen	HNRNPDL		1,10	0,28		1,08	0,29	4	4	3	12,1	12,1	9,9	40,04	0	31,783	998070000	70	A0A087WI	A0A087W	25,70	25,66	25,74	26,23	25,92	25,81	25,63	25,23	25,39
sp|P1698	Y-box-binc	YBX3	+	3,87	3,19		0,53	0,29	15	15	4	65,6	65,6	7,8	40,089	0	323,31	15483000000	190	P16989;P1	P16989;P1	30,28	30,52	29,97	30,89	30,30	30,43	26,75	27,25	27,17
tr|A0A0A	Plastin-3	PLS3		0,71	-0,72		0,17	0,28	5	5	5	8,3	8,3	8,3	69,334	0	30,883	121510000	11	A0A0A0M	A0A0A0M	22,90	22,28	22,40	23,52	23,26	21,65	23,73	23,59	22,41
sp|Q7Z2W	Zinc finger	ZC3HAV1	+	3,06	2,22		0,32	0,28	3	3	3	6,9	6,9	6,9	77,902	0	31,337	206440000	13	Q7Z2W4-2	Q7Z2W4-2	24,00	24,53	23,91	24,99	23,99	24,30	21,76	21,80	22,24
tr|J3QLS3	28S ribosa	MRPS7	+	1,37	2,33		0,46	0,27	6	6	6	22,1	22,1	22,1	31,704	0	41,582	737650000	25	J3QLS3;Q9	J3QLS3;Q9	25,64	26,21	25,59	26,34	26,12	25,79	24,18	24,33	21,95
sp|P4804	ATP synth	ATP5O		0,43	0,15		0,55	0,26	4	4	4	21,6	21,6	21,6	23,277	0	29,544	667160000	43	P48047;H7	P48047;H7	25,08	25,37	24,88	25,67	25,14	25,31	24,97	25,02	24,89
sp|P3194	14-3-3 pro	SFN		1,19	-0,69		0,09	0,25	13	13	10	47,2	47,2	37,1	27,774	0	145,81	5061600000	196	P31947;P3	P31947;P3	27,50	26,90	27,35	26,58	29,46	26,45	27,88	28,32	27,63
sp|O4370	Alpha-acti	ACTN4;ACTN2		0,01	0,00		0,38	0,25	6	6	1	9,4	9,4	2,7	104,85	0	65,924	372150000	10	O43707;O	O43707;O	23,99	24,06	24,39	24,31	24,85	24,02	23,96	24,36	24,12
sp|P5470	Sodium/pc	ATP1B3		0,30	0,61		0,14	0,24	2	2	2	10,4	10,4	10,4	31,512	0	11,525	149690000	5	P54709;H7	P54709;H7	23,56	23,82	21,88	23,27	23,55	23,15	22,48	23,42	21,53
sp|P3524	Replicatio	RFC4		0,92	0,87		0,54	0,23	4	4	4	20,9	20,9	20,9	39,681	0	37,446	105230000	8	P35249;C9	P35249;C9	23,14	23,12	23,42	23,45	23,73	23,18	21,83	22,04	23,21
tr|A0A087	ATP-depe	DDX50	+	2,23	1,54		0,31	0,22	4	3	3	7,4	5,3	5,3	82,226	0	20,44	83162000	10	A0A087W	A0A087W	22,70	23,31	23,08	23,49	23,44	22,81	21,05	21,83	21,58
sp|Q9966	Kinesin-lik	KIF2C	+	2,49	-0,41		0,55	0,21	3	3	3	6	6	6	75,561	0	19,744	91762000	16	Q99661-2;	Q99661-2;	22,35	22,36	22,28	22,64	22,21	22,76	22,76	22,63	22,84
sp|Q6PKG	La-related	LARP1	+	1,99	2,48		0,20	0,21	9	9	9	12,2	12,2	12,2	123,51	0	80,793	637300000	36	Q6PKG0;C	Q6PKG0;C	25,00	26,32	25,44	25,83	25,61	25,95	22,69	23,87	22,75
sp|P3194	14-3-3 pro	YWHAB	+	1,55	1,69		0,38	0,21	7	4	4	32,4	22,1	22,1	27,85	0	29,911	292160000	18	P31946-2;	P31946-2;	23,71	24,17	23,95	23,91	24,52	24,02	23,20	21,96	21,61
sp|P4678	40S ribosa	RPS10;RPS	+	2,16	4,52		0,26	0,19	12	12	12	60,6	60,6	60,6	18,898	0	209,12	9084900000	126	P46783;F6	P46783;F6	29,32	30,14	29,47	30,15	29,68	29,67	25,59	23,48	26,31
sp|P0508	Arginase-1	ARG1	+	2,36	-1,55		0,14	0,18	11	11	11	45,7	45,7	45,7	34,735	0	107,56	1931100000	80	P05089;P0	P05089;P0	25,65	25,59	26,31	25,56	25,61	26,93	27,66	27,21	27,33
sp|P6780	Nuclease-s	YBX1	+	3,17	4,05		0,36	0,18	13	10	10	53,1	43,2	43,2	35,924	0	323,31	9459800000	144	P67809;HC	P67809;HC	29,62	29,85	29,27	29,96	29,52	29,81	25,36	26,28	24,95
sp|P3194	Heterogen	HNRNPH3		0,28	0,57		0,79	0,18	3	3	3	11,8	11,8	11,8	35,238	0	21,3	590720000	16	P31942-2;	P31942-2;	24,89	24,95	24,81	25,26	25,01	24,93	25,15	22,70	25,10
tr|E7ETK0	40S ribosa	RPS24	+	2,69	5,86		0,34	0,18	5	5	5	35,9	35,9	35,9	15,197	0	60,496	4114300000	61	E7ETK0;A	E7ETK0;A	28,55	28,44	27,94	28,58	28,28	28,62	21,54	21,76	24,04
sp|Q9BRT	Protein LLI	LLPH	+	3,56	2,43		0,44	0,17	2	2	2	21,7	21,7	21,7	15,225	0	21,392	284010000	10	Q9BRT6	Q9BRT6	24,44	24,93	24,54	24,97	24,72	24,75	22,36	21,94	22,33
sp|Q96P6	Serpin B12	SERPINB12	+	1,93	-1,51		0,06	0,13	5	5	5	13,6	13,6	13,6	46,276	0	40,486	798130000	44	Q96P63;Q	Q96P63;Q	24,18	24,00	24,99	23,99	23,58	26,00	26,20	25,80	25,69
tr|Q5TEC6	Histone H3	HIST2H3PS	+	2,04	3,15		0,25	0,12	4	2	1	27,2	15,4	8,1	15,43	0	13,668	5773100000	40	Q5TEC6	Q5TEC6	29,10	29,28	28,77	29,40	28,99	29,12	26,51	24,61	26,59
sp|Q0146	Fatty acid-	FABP5	+	1,82	-1,22		0,10	0,12	4	4	4	25,2	25,2	25,2	15,164	0	33,566	3626400000	79	Q01469;K	Q01469	26,55	26,51	27,28	26,36	26,73	27,63	28,32	27,93	27,76
tr|J3QR29	Cyclin-dep	CDK11B;C	+	3,55	2,78		0,16	0,11	4	4	4	4,9	4,9	4,9	87,109	0	22,825	693630000	11	J3QR29;A	J3QR29;A	24,22	24,51	23,89	24,22	24,67	24,06	21,39	21,20	21,70
sp|Q0855	Desmocoll	DSC1		1,05	-1,12		0,05	0,11	10	10	10	15	15	15	93,834	0	109,75	3680800000	123	Q08554-2;	Q08554-2;	27,08	26,23	27,56	26,24	26,55	28,42	28,63	28,05	27,54
tr|A0A0C4	Zymogen g	ZG16B		0,49	-0,29		0,13	0,11	4	4	4	31,5	31,5	31,5	19,6	0	125,68	436600000	13	A0A0C4DC	A0A0C4DC	21,86	21,57	22,42	22,21	22,20	21,75	22,29	22,29	22,14
sp|P6813	Actin, alph	ACTA1;ACTC1;ACTG2		0,20	-0,16		0,09	0,10	13	1	1	31,3	4,2	4,2	42,051	0	44,659	4634100000	51	P68133;P6	P68133;P6	27,44	27,27	28,10	27,25	27,62	28,23	27,76	28,12	27,42
sp|Q96PK	RNA-bindi	RBM14		0,44	0,27		0,08	0,09	6	6	6	12,4	12,4	12,4	69,491	0	68,596	943500000	63	Q96PK6	Q96PK6	26,04	25,91	25,35	26,49	25,58	25,50	25,47	25,25	25,78
sp|Q1324	Serine/arg	SRSF5		0,94	1,27		0,23	0,08	3	2	2	12,5	9,2	9,2	31,263	0	14,09	158310000	11	Q13243;B	Q13243;B	23,69	23,83	23,66	23,65	24,03	23,73	23,57	22,42	21,38
tr|H3BQN	Fructose-b	ALDOA		0,03	-0,03		0,04	0,07	8	8	8	26,6	26,6	26,6	39,34	0	66,133	719350000	28	H3BQN4;J	H3BQN4;J	24,98	24,76	25,45	24,54	26,43	24,44	24,78	25,79	24,72
sp|P0408	Annexin A	ANXA1		1,09	-0,92		0,03	0,07	9	9	9	32,9	32,9	32,9	38,714	0	104,25	1115300000	47	P04083;Q	P04083;Q	24,59	24,92	25,84	24,36	26,47	24,74	26,02	26,25	25,82
tr|C9JJT5	ATP synth	ATP5J2-PTCD1;ATP5J2		0,73	-0,86		0,04	0,07	2	2	2	44,4	44,4	44,4	5,9149	0	14,857	251040000	24	C9JJT5;C9	C9JJT5;C9	24,18	22,52	24,10	23,99	23,74	23,26	24,48	24,38	24,52
sp|Q9H0S	Probable A	DDX47	+	2,33	-0,67		0,13	0,06	3	3	3	8,6	8,6	8,6	45,169	0	18,666	210900000	24	Q9H0S4-2,	Q9H0S4-2	23,45	23,33	23,43	23,77	23,42	23,21	23,85	24,18	24,20
tr|A0A087	Eukaryotic	EIF3H		0,97	0,72		0,05	0,05	2	2	2	9,5	9,5	9,5	39,589	0	15,144	81073000	9	A0A087W	A0A087W	22,64	22,72	22,53	23,08	22,02	22,94	22,37	22,13	21,25
sp|P0254	Prelamin-A	LMNA	+	1,86	-0,83		0,03	0,04	16	15	15	27,9	26,7	26,7	74,139	0	101,88	1234600000	65	P02545;P0	P02545;P0	25,46	25,55	25,58	25,24	26,59	24,89	26,52	26,60	25,98
sp|P09211	Glutathion	GSTP1	+	1,93	-1,48		0,02	0,04	4	4	4	22,4	22,4	22,4	23,356	0	45,883	864950000	47	P09211;A	P09211;A	24,37	24,49	25,18	23,93	25,92	24,30	26,02	26,59	25,85
sp|O6083	H/ACA ribo	DKC1	+	3,32	2,74		0,14	0,04	5	5	5	14,4	14,4	14,4	57,673	0	46,392	343660000	27	O60832;C	O60832;C	24,88	25,14	24,80	25,05	24,94	24,94	22,65	21,83	22,12
sp|O7536	Core histo	H2AFY	+	2,93	3,87		0,03	0,04	8	8	8	33,6	33,6	33,6	39,183	0	164,52	2487300000	74	O75367-2;	O75367-2;	27,76	28,49	27,22	28,10	27,56	27,91	23,91	23,46	24,47
sp|P0404	Catalase	CAT		1,29	-0,99		0,02	0,02	6	6	6	15,4	15,4	15,4	59,755	0	53,716	656760000	41	P04040	P04040	24,59	24,37	24,97	24,63	23,93	25,43	26,24	25,50	25,17
sp|Q0894	FACT com	SSRP1	+	3,03	3,67		0,03	0,02	7	7	7	11,4	11,4	11,4	81,074	0	74,584	760670000	45	Q08945;A	Q08945	26,03	26,62	25,98	26,48	26,09	26,12	22,08	22,27	23,26
sp|P5045	Serpin H1	SERPINH1	+	2,04	-1,19		0,02	0,02	2	2	2	6,7	6,7	6,7	46,44	0	15,849	92677000	15	P50454;H	P50454;H	22,47	22,06	22,53	21,97	22,58	22,56	23,45	23,93	23,25
tr|M0R0Y	RuvB-like 2	RUVBL2	+	1,36	0,74		0,02	0,01	4	4	4	15,5	15,5	15,5	38,755	0	26,866	274830000	23	M0R0Y3;C	M0R0Y3;C	24,22	24,44	23,88	24,49	24,07	24,02	23,26	23,83	23,23
tr|A0A087	Heterogen	HNRNPM		0,06	-0,02		0,02	0,01	19	19	19	31,9	31,9	31,9	77,569	0	217,25	4244100000	227	A0A087X0	A0A087X0	28,06	27,85	27,73	28,32	27,80	27,57	28,01	27,97	27,73
sp|Q9BVA	Tubulin be	TUBB2B;TUBB2A		0,61	-1,03		0,00	0,00	13	2	2	37,3	5,4	5,4	49,953	0	13,895	233520000	20	Q9BVA1;C	Q9BVA1;C	23,06	22,18	22,57	22,39	22,07	21,03	24,37	24,33	22,20
sp|Q8NHL	Cancer/te	CT45A3;C	+	1,44	1,64		0,00	0,00	3	3	3	16,9	16,9	16,9	21,33	0	20,024	269660000	16	Q8NHU0;C	Q8NHU0;C	24,57	24,62	24,31	24,57	24,58	24,35	22,12	23,87	22,57
sp|Q9Y3I0	tRNA-splic	RTCB	+	1,85	-0,39		0,02	-0,01	5	5	5	15,8	15,8	15,8	55,21	0	37,102	398790000	20	Q9Y3I0	Q9Y3I0	24,63	24,59	24,37	24,77	24,41	24,38	24,94	24,99	24,83
tr|F8W727	60S ribosa	RPL32	+	2,45	3,07		0,01	-0,01	5	5	5	24,2	24,2	24,2	17,962	0	35,616	1964400000	32	F8W727;P	F8W727;P	27,66	26,43	27,56	27,25	27,05	27,34	24,46	23,54	24,45
sp|P62316	Small nucl	SNRPD2	+	3,06	3,84		0,02	-0,01	4	4	4	37,3	37,3	37,3	13,527	0	25,938	682480000	18	P62316;K7	P62316;K7	25,70	25,97	25,80	26,12	25,64	25,69	22,42	21,14	22,39
sp|P2273	Protein-gl	TGM1		0,94	-2,13		0,00	-0,01	6	6	6	8,8	8,8	8,8	89,786	0	36,677	223600000	10	P22735;P2	P22735;P2	20,39	22,04	24,04	21,88	21,52	23,04	24,32	24,18	24,37
sp|P2782	Calnexin	CANX		0,18	0,09		0,03	-0,02	6	6	6	12,7	12,7	12,7	67,567	0	41,025	851020000	43	P27824;P2	P27824;P2	25,53	25,86	25,50	25,71	25,83	25,29	25,56	25,78	25,29
sp|Q9252	Histone H1	H1FX	+	3,76	3,49		0,04	-0,02	4	4	4	18,3	18,3	18,3	22,487	0	30,737	665640000	36	Q92522	Q92522	25,90	26,14	26,04	26,27	25,89	25,87	22,79	22,78	22,04
sp|P8407	ADP-ribos	ARF1;ARF	+	1,32	-0,62		0,03	-0,02	5	5	3	35,9	35,9	18,2	20,697	0	38,229	1609100000	61	P84077;P6	P84077;P6	26,55	25,97	26,09	26,19	26,22	26,14	26,78	27,08	26,62
sp|Q9Y5B	FACT com	SUPT16H	+	3,90	4,59		0,02	-0,02	8	8	8	9,8	9,8	9,8	119,91	0	62,723	922450000	40	Q9Y5B9	Q9Y5B9	26,31	26,99	26,16	26,59	26,48	26,32	21,75	22,25	21,68
sp|P4093	Replicatio	RFC3	+	3,26	0,50		0,09	-0,03	2	2	2	9,2	9,2	9,2	34,756	0	15,815	120750000	15	P40938-2;	P40938-2;	22,91	22,90	22,77	23,02	22,76	22,73	22,36	22,40	22,34
tr|A0A087	Tropomyo	TPM3;DKFZp686J1372		0,51	-0,42		0,03	-0,03	7	7	4	26,4	26,4	16,7	26,42	0	60,234	936450000	40	A0A087W	A0A087W	25,77	24,99	25,59	25,38	25,67	25,21	26,37	25,81	25,43
sp|O1498	Exportin-1	XPO1		0,15	0,29		0,04	-0,03	2	2	2	1,7	1,7	1,7	123,38	0	12,027	62441000	4	O14980;C	O14980;C	22,36	22,50	22,07	22,24	22,58	22,04	23,28	21,94	20,84
sp|P0187	Ig alpha-1	IGHA1;IGHA2		0,98	-0,92		0,01	-0,03	7	7	7	21	21	21	37,654	0	45,11	529660000	11	P01876;A	P01876;A	22,44	23,69	23,74	21,85	23,89	24,05	24,41	24,10	24,12
sp|P0781	Bifunction	EPRS		1,13	-0,31		0,11	-0,03	3	3	3	2,5	2,5	2,5	170,59	0	18,288	264920000	25	P07814;V	P07814	23,66	23,95	23,80	23,83	23,84	23,64	23,91	24,20	24,22
tr|B9A067	MICOS cor	IMMT	+	6,77	3,27		0,10	-0,04	4	4	4	7,2	7,2	7,2	78,973	0	22,265	459750000	3	B9A067;Q	B9A067;Q	25,37	25,23	25,29	25,13	25,10	25,54	22,00	22,03	22,05
sp|P1363	Elongation	EEF2	+	1,48	-0,34		0,05	-0,05	14	14	14	17,1	17,1	17,1	95,337	0	113,49	2992500000	149	P13639	P13639	27,32	27,20	27,06	27,29	27,57	26,58	27,59	27,63	27,38
sp|P6310	14-3-3 pro	YWHAZ		0,59	-0,41		0,03	-0,05	9	6	6	40	29,8	29,8	27,745	0	246,13	1839300000	83	P63104;E7	P63104;E7	25,99	26,00	26,31	25,64	27,09	25,40	26,18	27,08	26,24
tr|H0YLA2	Signal rec	SRP14		0,78	1,75		0,30	-0,05	2	2	2	23,5	23,5	23,5	13,058	0	17,789	476070000	21	H0YLA2;P	H0YLA2;P	24,82	24,68	24,67	24,69	24,75	24,57	21,68	25,03	22,22
sp|O6026	SWI/SNF-r	SMARCA5	+	3,42	3,98		0,11	-0,06	12	12	12	12,5	12,5	12,5	121,9	0	78,272	663620000	48	O60264;A	O60264	25,84	26,37	25,88	26,06	26,03	25,82	22,56	21,47	22,12
tr|A0A0R4	Matrin-3	MATR3		0,74	0,23		0,12	-0,06	14	14	14	22,7	22,7	22,7	94,622	0	232,2	2223200000	90	A0A0R4I2	A0A0R4I2	27,13	27,15	26,82	27,26	26,91	26,74	26,62	26,93	26,86
sp|Q96FQ	Protein S1	S100A16	+	1,75	-0,50		0,08	-0,06	3	3	3	33	33	33	11,801	0	21,812	340120000	39	Q96FQ6	Q96FQ6	24,11	24,10	23,89	24,44	23,92	23,55	24,75	24,42	24,43
sp|P0474	Alpha-amy	AMY1A;AMY1B;AMY2		0,88	-0,54		0,10	-0,07	4	4	4	11,7	11,7	11,7	57,767	0	44,352	146410000	13	P04745;Q	P04745;Q	22,91	22,15	22,44	22,45	22,19	22,65	23,07	23,33	22,72
sp|P0055	Phosphogl	PGK1		0,23	-0,66		0,02	-0,08	4	4	4	15,2	15,2	15,2	41,428	0	28,839	292970000	13	P00558-2;	P00558-2;	22,71	21,75	24,53	21,48	24,40	22,89	22,30	24,97	23,71
sp|P1059	Thioredox	TXN	+	2,80	-1,29		0,11	-0,08	5	5	5	42,9	42,9	42,9	11,737	0	49,055	4731700000	106	P10599;P1	P10599;P1	27,63	27,22	27,41	27,30	26,92	27,79	28,91	28,72	28,49
tr|U3KQK	Histone H2	HIST1H2B	+	2,95	2,74		0,19	-0,09	8	8	2	40,4	40,4	6	18,804	0	323,31	78095000000	187	U3KQK0;C	U3KQK0;C	32,51	32,74	32,38	32,74	32,37	32,26	29,93	29,22	30,28
sp|P1933	Nucleolin	NCL	+	2,03	3,49		0,14	-0,09	22	22	22	29,6	29,6	29,6	76,613	0	323,31	12089000000	190	P19338;H7	P19338;H7	30,07	30,56	29,86	30,29	29,87	30,06	27,16	25,27	27,60
tr|J3QS39	Ubiquitin-	UBB;RPS27A;UBC;UBA		0,78	-0,33		0,32	-0,10	3	3	3	36,6	36,6	36,6	10,469	0	42,319	2451700000	66	J3QS39;J3	J3QS39;J3	27,10	26,94	26,98	27,11	26,89	26,73	27,06	27,69	27,25
sp|P3193	Cytochrom	UQCRC1	+	1,78	2,12		0,22	-0,10	2	2	2	6,7	6,7	6,7	52,645	0	24,679	215240000	9	P31930	P31930	24,20	24,23	24,01	24,11	24,29	23,73	21,32	21,69	23,06
tr|C9J9K3	40S ribosa	RPSA	+	3,28	4,07		0,15	-0,11	3	3	3	14,4	14,4	14,4	29,404	0	28,57	455290000	23	C9J9K3;A	C9J9K3;A	25,48	25,59	25,37	25,40	25,80	24,93	21,67	20,64	21,94
tr|A0A1B	Glutamine	QARS		0,29	0,38		0,08	-0,11	5	5	5	8	8	8	83,782	0	32,253	562390000	13	A0A1B0G	A0A1B0G	24,70	24,75	25,83	24,56	25,58	24,83	24,29	25,49	24,35
tr|E7EQR	Ezrin	EZR		0,57	0,40		0,09	-0,11	6	6	6	9	9	9	69,371	0	36,392	298060000	15	E7EQR4;P	E7EQR4;P	23,82	23,96	24,73	23,90	24,66	23,62	23,58	24,04	23,68
sp|Q9NS6	Mitochonc	TOMM22	+	1,60	1,45		0,07	-0,11	2	2	2	16,2	16,2	16,2	15,521	0	67,176	411070000	23	Q9NS69	Q9NS69	24,79	25,73	24,44	25,61	24,54	24,48	23,34	23,84	23,43
sp|Q9945	Cell divisio	CDC5L	+	1,65	1,84		0,25	-0,12	3	3	3	5,9	5,9	5,9	92,25	0	17,543	139610000	9	Q99459	Q99459	23,53	23,50	24,00	23,61	23,39	23,69	21,60	21,15	22,77
tr|K7EMV	Histone H3	H3F3B;H3	+	2,63	3,02		0,13	-0,12	5	5	3	35,9	35,9	10,9	10,334	0	36,964	39648000000	83	K7EMV3;E	K7EMV3;E	31,97	32,20	31,37	32,19	31,58	31,43	28,67	28,30	29,52
sp|P3194	Stress-ind	STIP1		0,14	0,21		0,28	-0,12	2	2	2	3,9	3,9	3,9	59,777	0	12,609	161780000	18	P31948-3;	P31948-3;	23,22	22,80	23,37	22,99	23,04	23,00	23,28	23,60	21,89
sp|Q9P0L	Vesicle-as	VAPA		0,16	-0,06		0,17	-0,12	4	4	4	21,3	21,3	21,3	27,893	0	30,264	413640000	27	Q9P0L0;C	Q9P0L0;C	24,69	24,58	24,33	24,53	24,75	23,96	24,49	24,50	24,80
sp|P6280	Histone H4	HIST1H4A	+	2,81	2,89		0,16	-0,12	10	10	10	60,2	60,2	60,2	11,367	0	129,51	2,3259E+11	248	P62805	P62805	34,37	34,80	34,03	34,64	34,15	34,06	31,58	30,96	32,01
sp|P4270	Leucine-ric	LRPPRC		0,30	-0,10		0,24	-0,12	5	5	5	4	4	4	157,9	0	29,838	377070000	12	P42704;B	P42704	24,32	24,41	24,52	24,59	24,36	23,93	24,53	24,70	24,30
tr|A0A0C4	Cullin-asso	CAND1	+	2,22	-0,53		0,25	-0,12	5	5	5	8,1	8,1	8,1	85,408	0	30,752	383960000	19	A0A0C4DC	A0A0C4DC	24,55	24,31	24,42	24,05	24,66	24,20	25,08	24,83	24,95
sp|P5259	Heterogen	HNRNPF		0,23	0,06		0,53	-0,13	9	9	7	29,2	29,2	22,7	45,671	0	98,483	2577600000	137	P52597;A	P52597	27,48	27,29	27,16	27,27	27,16	27,12	27,15	27,34	27,25
sp|Q1476	Major vau	MVP		0,98	-0,49		0,17	-0,13	4	4	4	5,6	5,6	5,6	99,326	0	24,623	183380000	16	Q14764;H	Q14764;H	23,61	23,03	22,92	22,78	23,43	22,95	23,69	23,84	23,50
sp|P5588	Eukaryotic	EIF3B		1,17	0,82		0,19	-0,13	3	3	3	4,4	4,4	4,4	92,48	0	21,9	210300000	21	P55884;P5	P55884;P5	23,70	24,22	23,74	23,90	24,01	23,36	22,51	23,42	23,28
sp|Q1618	Proteasom	ADRM1		0,32	0,15		0,17	-0,13	2	2	2	5,9	5,9	5,9	42,153	0	11,936	70512000	5	Q16186;A	Q16186;A	22,36	22,95	22,49	22,20	22,92	22,29	22,55	22,33	22,48
sp|P0723	Protein dis	P4HB		0,69	-0,74		0,05	-0,13	7	7	7	15,4	15,4	15,4	57,116	0	52,605	476050000	36	P07237;H	P07237;H	24,16	23,88	24,69	23,76	25,65	22,92	25,09	25,68	24,20
sp|O0030	Eukaryotic	EIF3F		1,25	0,95		0,15	-0,14	5	5	5	18,5	18,5	18,5	37,563	0	41,674	424920000	27	O00303;H	O00303	24,35	25,31	25,04	24,96	24,96	24,34	23,82	24,37	23,66
sp|O9600	Mitochonc	TOMM40	+	1,36	1,93		0,21	-0,15	3	3	3	12,5	12,5	12,5	34,441	0	20,163	245880000	11	O96008-2;	O96008-2;	24,19	24,41	24,51	24,73	24,07	23,86	22,57	23,50	21,24
sp|P2734	14-3-3 pro	YWHAQ		0,30	0,16		0,23	-0,15	8	5	5	31,8	21,6	21,6	27,764	0	84,897	1172600000	49	P27348;E9	P27348;E9	26,32	26,30	25,73	26,32	25,85	25,74	25,82	26,14	25,92
sp|P8160	Dermcidin	DCD	+	1,53	-1,11		0,14	-0,15	4	4	4	35,5	35,5	35,5	11,284	0	30,583	1335100000	55	P81605;P8	P81605;P8	25,42	25,12	26,06	25,91	24,87	25,36	27,01	26,47	26,45
tr|E7ERS3	Zinc finger	ZC3H18	+	1,83	1,77		0,41	-0,15	6	6	6	8	8	8	108,94	0	56,634	505420000	33	E7ERS3;C	E7ERS3;C	25,51	25,51	25,34	25,42	25,00	25,48	22,83	24,03	24,18
tr|A0A087	Polyadeny	PABPC1;PABPC3		0,02	-0,07		0,05	-0,16	3	3	3	6,9	6,9	6,9	58,535	0	24,267	142690000	11	A0A087W	A0A087W	21,48	23,18	24,01	23,37	23,57	21,26	23,62	23,51	21,75
sp|Q0902	Histone-bi	RBBP4;RBI	+	1,91	0,77		0,30	-0,16	5	5	5	12,4	12,4	12,4	46,158	0	33,03	984130000	19	Q09028-3;	Q09028-3;	25,93	26,52	26,14	26,28	25,97	25,87	25,34	25,43	25,51
sp|Q96ST	Protein IW	IWS1	+	1,70	1,87		0,30	-0,16	4	4	4	8,1	8,1	8,1	56,109	0	22,022	108830000	8	Q96ST2-2;	Q96ST2-2;	23,31	23,87	23,20	23,34	23,39	23,17	22,46	21,36	20,94
sp|P5507	Transition	VCP		0,24	-0,28		0,10	-0,16	10	10	10	15,1	15,1	15,1	89,321	0	73,127	790540000	32	P55072;C9	P55072	25,13	25,14	25,55	24,77	26,22	24,34	25,38	26,36	24,91
sp|P0479	Heat shock	HSPB1	+	2,07	-0,70		0,40	-0,17	12	12	12	77,6	77,6	77,6	22,782	0	271,44	15203000000	242	P04792;F8	P04792;F8	29,28	29,26	29,50	29,10	29,48	28,96	29,97	30,29	29,88
sp|P1798	T-complex	TCP1		0,11	0,06		0,42	-0,17	4	4	4	10,8	10,8	10,8	60,343	0	22,686	224550000	7	P17987;F5	P17987;F5	23,78	23,66	24,04	23,57	23,92	23,48	23,80	24,01	23,50
tr|F1T0B3	ATP-depe	DDX1	+	1,44	-0,39		0,49	-0,18	4	4	4	9,1	9,1	9,1	73,915	0	39,086	293980000	20	F1T0B3;A	F1T0B3;A	24,00	24,21	23,79	23,87	23,96	23,64	24,34	24,37	24,46
sp|Q9UD	Cytochrom	UQCR10		0,38	0,14		0,86	-0,18	2	2	2	38,1	38,1	38,1	7,3084	0	18,079	434200000	25	Q9UDW1;	Q9UDW1;	24,70	24,67	24,83	24,71	24,51	24,44	24,88	24,40	24,51
sp|Q0032	Phosphate	SLC25A3		0,43	0,11		0,22	-0,18	6	6	6	17,2	17,2	17,2	39,958	0	38,655	1567800000	78	Q00325-2;	Q00325-2;	26,76	26,53	26,40	26,91	26,37	25,87	26,43	26,50	26,42
tr|X6R700	Chromatin	CHTOP	+	3,88	3,22		0,21	-0,18	3	3	3	18,8	18,8	18,8	23,661	0	36,774	470330000	16	X6R700;C	X6R700;C	25,52	25,86	25,34	25,88	25,44	24,85	22,23	22,68	22,16
sp|Q9Y22	UPF0568 p	C14orf166		1,15	-0,33		0,30	-0,19	5	5	5	24,2	24,2	24,2	28,068	0	36,955	263960000	23	Q9Y224;G	Q9Y224;G	23,94	23,79	24,05	23,29	24,12	23,81	24,08	24,46	24,21
sp|P0040	Cytochrom	MT-CO2		0,69	0,89		0,23	-0,19	2	2	2	13,2	13,2	13,2	25,565	0	20,226	280700000	32	P00403	P00403	24,02	24,42	24,10	23,76	24,59	23,62	22,39	24,36	23,12
tr|A0A0U	RNA-bindi	RBM39		0,06	-0,02		0,42	-0,19	8	8	8	40,4	40,4	40,4	26,698	0	58,477	1133100000	46	A0A0U1RC	A0A0U1RC	26,12	26,12	25,99	26,19	25,92	25,53	26,02	26,34	25,93
sp|Q9NXF	Testis-exp	TEX10	+	3,66	3,21		0,50	-0,20	8	8	8	11,9	11,9	11,9	103,91	0	79,409	607050000	21	Q9NXF1-2	Q9NXF1-2	25,69	26,26	25,89	25,71	25,73	25,81	22,87	22,37	22,98
sp|Q96AG	Leucine-ric	LRRC59		1,16	0,40		0,40	-0,20	5	5	5	18,9	18,9	18,9	34,93	0	47,855	1295800000	83	Q96AG4	Q96AG4	26,38	26,66	26,22	26,51	26,20	25,96	26,18	26,04	25,85
sp|P1781	CTP synth	CTPS1		1,25	-0,48		0,34	-0,20	10	10	10	21	21	21	66,69	0	87,971	1680800000	106	P17812;P1	P17812;P1	26,77	26,39	26,19	26,51	26,32	25,94	26,96	27,02	26,82
sp|P1486	Heterogen	HNRNPL	+	2,52	-0,68		0,44	-0,20	7	7	7	22,2	22,2	22,2	64,132	0	85,23	1337900000	73	P14866;M	P14866;M	26,25	26,07	25,93	26,11	26,00	25,55	26,67	26,80	26,84
sp|P0408	Cystatin-B	CSTB	+	2,81	-1,58		0,30	-0,20	3	3	3	45,9	45,9	45,9	11,139	0	19,905	469160000	25	P04080	P04080	23,61	23,47	23,37	23,78	22,90	23,18	25,45	24,84	24,91
tr|D6RFM	Succinate	SDHA		0,95	-2,18		0,06	-0,20	2	2	2	4,1	4,1	4,1	63,566	0	15,289	229500000	7	D6RFM5;P	D6RFM5;P	21,80	24,72	21,24	22,28	22,93	21,95	24,81	24,79	24,71
sp|P3211	Peroxiredo	PRDX2	+	2,65	-1,32		0,58	-0,20	7	6	6	32,3	26,8	26,8	21,892	0	55,6	2817200000	147	P32119;A	P32119;A	26,88	26,57	26,73	26,69	26,27	26,61	29,28	28,15	27,72
sp|P5114	Ras-relate	RAB7A		0,49	0,17		0,24	-0,21	7	7	7	36,2	36,2	36,2	23,489	0	62,073	1277500000	42	P51149;C9	P51149;C9	26,45	26,43	26,15	26,65	26,22	25,54	26,33	26,25	25,94
tr|E7ENN	Nesprin-1	SYNE1		0,38	1,22		1,15	-0,21	4	4	4	0,6	0,6	0,6	964,83	0	25,004	540890000	10	E7ENN3;A	E7ENN3;A	25,13	25,20	24,95	24,98	24,84	24,84	21,17	25,30	25,15
sp|P0484	Dolichyl-d	RPN1		1,05	0,52		0,35	-0,22	14	14	14	27,7	27,7	27,7	68,569	0	113,34	1808500000	109	P04843;B7	P04843;B7	27,10	27,05	26,63	26,96	26,88	26,29	26,14	26,75	26,34
sp|P5229	Importin s	KPNA2		1,29	0,47		0,35	-0,22	11	11	11	26,3	26,3	26,3	57,861	0	186,75	1901700000	103	P52292;J3	P52292	27,00	27,24	26,73	27,17	26,69	26,44	26,46	26,41	26,68
sp|P0555	Integrin be	ITGB1		0,37	0,75		0,90	-0,22	2	2	2	3,4	3,4	3,4	87,445	0	11,492	203590000	6	P05556-2;	P05556-2;	23,42	23,67	23,78	23,49	23,37	23,35	23,66	23,77	21,18
sp|P1784	Probable A	DDX5	+	1,55	-0,35		0,58	-0,22	21	21	17	38,3	38,3	31,1	69,147	0	181,83	16437000000	445	P17844;J3	P17844;J3	29,90	29,80	29,67	29,84	29,56	29,30	30,22	30,21	29,98
sp|P3010	Protein dis	PDIA3		0,85	-0,51		0,22	-0,22	4	4	3	11,3	11,3	9,1	56,782	0	26,09	345450000	16	P30101	P30101	24,06	23,71	24,52	23,60	24,50	23,52	24,48	24,91	24,43
sp|P6214	Serine/thr	PPP1CB;PF	+	1,84	1,66		0,59	-0,22	4	4	4	14,7	14,7	14,7	37,186	0	40,579	203530000	15	P62140;C9	P62140;C9	24,37	24,11	24,35	23,85	24,34	23,97	22,69	23,26	21,91
sp|Q1457	Desmocoll	DSC3	+	1,86	-1,54		0,05	-0,23	6	6	6	12	12	12	93,453	0	106,04	998060000	31	Q14574-2;	Q14574-2;	24,67	24,41	24,92	21,67	24,88	26,79	26,87	25,77	25,99
sp|Q1375	Laminin su	LAMB3		0,49	-0,57		0,11	-0,23	4	4	4	4,9	4,9	4,9	129,57	0	31,231	166630000	18	Q13751;X	Q13751	21,93	23,67	23,08	23,53	22,93	21,51	23,37	23,57	23,46
sp|P6810	Elongation	EEF1A1;EE	+	1,38	-0,50		0,39	-0,23	13	13	4	35,5	35,5	12,6	50,14	0	207,51	75901000000	426	P68104;Q	P68104;Q	32,09	31,88	31,54	31,96	31,54	31,32	32,39	32,37	32,25
sp|P0673	Alpha-eno	ENO1		1,19	-1,43		0,13	-0,23	7	7	7	19,1	19,1	19,1	47,168	0	59,449	801570000	66	P06733;K7	P06733;K7	23,97	24,33	25,69	23,65	24,94	24,71	26,05	26,47	25,75
sp|Q0966	Neuroblas	AHNAK		1,05	-0,32		0,49	-0,23	38	38	38	20,3	20,3	20,3	629,09	0	306,3	6371400000	232	Q09666;E	Q09666	28,46	28,07	28,52	28,11	28,39	27,85	28,71	28,72	28,60
sp|Q1324	Serine/arg	SRSF6	+	2,44	3,31		0,36	-0,24	3	3	1	9	9	2,7	38,418	0	22,921	509980000	26	Q13247-3;	Q13247-3	25,40	25,91	25,47	25,73	24,97	25,37	21,64	21,90	23,31
sp|Q9BUF	Tubulin be	TUBB6		0,95	0,18		0,50	-0,24	15	10	6	46	35	23,5	49,857	0	135,56	4327200000	159	Q9BUF5;K	Q9BUF5;K	28,13	28,04	28,03	27,88	28,15	27,45	27,77	28,05	27,86
tr|F5GWF	T-complex	CCT2		0,28	-0,09		0,38	-0,24	5	5	5	13,4	13,4	13,4	56,806	0	44,897	661060000	16	F5GWF6;P	F5GWF6;P	25,26	25,26	25,51	25,60	24,86	24,84	25,54	25,24	25,51
sp|P0674	Nucleophc	NPM1	+	4,68	3,79	+	2,39	-0,24	11	11	11	39,8	39,8	39,8	32,575	0	323,31	14038000000	145	P06748;P0	P06748;P0	30,41	30,52	30,42	30,22	30,16	30,23	26,62	26,40	26,95
tr|B0QY8	Eukaryotic	EIF3L	+	1,99	0,59		0,40	-0,24	2	2	2	3,5	3,5	3,5	70,901	0	13,781	86021000	6	B0QY89;Q	B0QY89;Q	22,76	23,16	23,05	22,98	22,98	22,29	22,49	22,33	22,37
sp|Q1539	Splicing fa	SF3B3	+	2,18	0,99		0,66	-0,24	11	11	11	12,5	12,5	12,5	135,58	0	83,832	694320000	30	Q15393;Q	Q15393	25,66	25,57	25,47	25,54	25,41	25,02	24,93	24,49	24,32
sp|P0773	Profilin-1	PFN1		0,45	-0,32		0,25	-0,25	5	5	5	42,9	42,9	42,9	15,054	0	39,805	912610000	48	P07737;K7	P07737;K7	25,68	24,99	25,77	25,15	25,80	24,74	25,85	26,07	25,47
tr|K7ENG	Splicing fa	U2AF2	+	1,78	-0,75		0,54	-0,25	3	3	3	11,1	11,1	11,1	33,901	0	18,062	315480000	28	K7ENG2;P	K7ENG2;P	23,91	23,94	23,71	23,74	23,84	23,23	24,61	24,91	24,30
sp|Q1389	Bystin	BYSL	+	2,69	3,79		0,34	-0,25	5	5	5	12,4	12,4	12,4	49,601	0	35,303	348390000	23	Q13895;H	Q13895	25,28	25,73	24,78	25,23	25,06	24,74	20,89	22,37	21,15
sp|Q1314	TAR DNA-l	TARDBP		0,19	-0,09		0,42	-0,26	5	5	5	17,1	17,1	17,1	44,739	0	40,515	568850000	32	Q13148;K	Q13148;K	25,23	25,17	24,67	25,15	24,54	24,61	25,18	24,99	25,17
tr|H0Y8C6	Importin-5	IPO5		0,04	-0,01		0,42	-0,26	4	4	4	4	4	4	123,75	0	24,084	214620000	19	H0Y8C6;O	H0Y8C6;O	23,78	23,95	23,90	24,02	23,69	23,14	24,02	23,83	23,81

(+) C9ET12 Prolifin-2	PFN2		0,81	-0,30	+	1,31	-0,46	5	2	2	51,6	19,9	19,9	9,7992	0	12,91	599590000	25	C9ET12;P3	C9ET12;P3	25,19	25,28	25,15	25,03	24,68	24,35	25,83	25,19	25,22
(+) P07742 Keratin, ty	EET1B		0,23	0,16		1,00	-0,48	12	10	9	21,9	19,1	16,4	49,057	0	10,249	1755000000	92	P07742;P4	P07742;P4	17,19	16,70	16,58	16,63	16,12	15,91	16,34	16,66	17,00
(+) P07737 Protein de	PARE7	+	1,76	-1,39	+	1,51	-0,60	4	4	4	21,9	21,9	21,9	19,991	0	17,212	913500000	35	Q96HT5;Q	Q96HT5;Q	15,42	15,07	15,45	14,91	14,71	14,60	16,39	16,65	16,20
(+) P30626 38S r Ikaso	MRPS22	+	3,10	3,84	+	1,77	-0,61	5	5	5	20,6	20,6	20,6	20,116	0	47,87	3490600000	17	P82662;E7	P82662;E7	25,62	25,72	25,23	24,97	24,85	24,94	21,47	22,65	21,14
(+) P30419 Caspase-1	CASP1P	+	1,22	-1,90		0,44	-0,61	10	10	10	26,2	26,2	26,2	27,679	0	79,947	1124000000	74	P10966	P10966	24,52	24,25	24,09	24,44	24,27	24,02	27,16	26,87	26,24
(+) P07960 Bisomycin	BLM		0,47	-0,38		0,94	-0,61	1	1	1	1,8	1,8	1,8	144,47	0,000128	7,3867	11123000000	24	P07960;P	P07960;P	29,27	29,48	29,46	29,31	28,77	28,30	29,33	29,86	29,57
(+) Q09732 3BS r Ikaso	MRPS28	+	2,33	2,71	+	1,58	-0,61	5	5	4	23,5	23,5	18,2	20,843	0	29,569	2601100000	24	Q9Y5Q8;H	Q9Y5Q8;H	24,87	25,24	24,68	24,58	24,58	24,23	22,36	21,32	22,95
(+) P61326 Protein ro	MAGOHA	+	2,24	2,51	+	2,06	-0,62	4	4	4	40,4	40,4	40,4	12,848	0	15,219	2732500000	14	P61326-2;	P61326-2;	24,91	24,97	25,10	24,54	24,55	24,48	20,90	22,71	22,14
(+) Q01470 Lemin-1 a	LIR		1,05	0,94		1,26	-0,62	4	4	4	9,1	9,1	9,1	79,701	0	15,766	1539100000	11	Q14739;C	Q14739;C	23,71	23,75	23,46	23,39	22,65	23,03	22,67	23,02	22,42
(+) Q09130 2BS r Ikaso	MRPS23	+	2,72	2,53		1,13	-0,62	4	4	4	25,3	25,3	25,3	21,77	0	15,175	1634500000	24	Q9Y3D9;C	Q9Y3D9;C	25,12	25,62	25,29	24,92	25,05	24,80	23,06	21,86	23,20
(+) Q08410 Reactin	ETN1		0,67	1,08		0,24	-0,62	3	3	3	3,2	3,2	3,2	149,61	0	18,844	2786600000	7	Q96EP2-2	Q96EP2-2	24,16	23,82	23,90	23,92	23,92	24,26	22,09	24,18	22,21
(+) C9EQ17 Prolifin-1	PFN1	+	1,12	-0,93		0,69	-0,62	5	5	2	51,7	51,7	20,9	9,9492	0	43,231	2283900000	65	C9EQ17;G5	C9EQ17;G5	27,11	26,57	26,67	26,87	26,01	25,58	27,92	27,81	27,55
(+) P49750 Transmer	TMED10		0,26	0,21		0,87	-0,66	3	3	3	11,7	11,7	11,7	34,976	0	19,584	1948000000	15	P49755;G5	P49755;G5	23,96	23,72	23,51	23,79	23,70	23,63	23,24	23,93	23,17
(+) Q07224 Rego iens	POGZ	+	1,35	2,03	+	1,69	-0,66	7	7	7	7,2	7,2	7,2	145,29	0	62,166	7376500000	23	Q7Z3K3-5;	Q7Z3K3-5;	25,72	26,22	25,97	25,51	25,25	25,18	22,20	21,58	22,99
(+) A0A087 Serine/arg	HSPF1	+	4,24	2,46	+	2,44	-0,67	6	6	5	43,1	43,1	43,1	15,763	0	61,24	3470200000	69	A0A087X1;	A0A087X1;	28,15	28,17	27,93	27,35	27,45	27,24	25,83	25,49	25,64
(+) Q00158 Hydroxym	HMGCS1		0,07	0,12		0,84	-0,67	3	3	3	10,6	10,6	10,6	57,293	0	19,621	2543900000	15	Q01581	Q01581	24,13	23,60	23,94	23,68	24,06	22,82	24,25	24,47	22,68
(+) Q16479 Nadh-ubiq	NDUFA9		0,22	0,24	+	1,47	-0,67	2	2	2	9	9	9	42,509	0	12,284	1176200000	12	Q16795;5T	Q16795;5T	22,11	22,07	22,15	22,68	22,61	22,02	22,23	22,18	22,12
(+) P31150 Endosmy	MA71A	+	1,70	-1,46		0,49	-0,68	4	4	4	11,2	11,2	11,2	43,66	0	15,019	1996500000	19	P31150;P3	P31150;P3	22,50	22,82	22,45	23,19	22,84	22,72	24,67	24,65	23,84
(+) Q09650 Eukaryoti	EIF4B		0,83	-0,98		0,75	-0,68	3	3	3	8,4	8,4	8,4	46,971	0	21,507	2658700000	19	Q09650	Q09650	24,19	23,96	23,80	23,30	23,17	22,61	24,01	25,31	24,64
(+) P52209 Chromodo	CHDGCHD	+	1,84	2,10	+	1,80	-0,70	5	5	5	3,1	3,1	3,1	217,1	0	10,664	1321100000	12	P52209;5	P52209;5	24,64	25,03	24,52	24,15	23,89	24,06	23,25	22,68	23,29
(+) Q06730 Pre-mRNA	PRPF8	+	1,99	2,21		0,64	-0,72	6	6	6	3,9	3,9	3,9	273,6	0	15,259	1296500000	15	Q6P02B;Q	Q6P02B;Q	24,28	24,84	24,45	24,73	23,52	23,15	21,85	23,22	21,87
(+) Q06124 Chromodo	CHAMP1	+	2,86	2,99	+	1,89	-0,73	5	5	5	7,3	7,3	7,3	89,098	0	18,713	2923500000	19	Q96JM3;5	Q96JM3;5	25,51	25,81	25,66	24,82	25,22	24,75	22,43	22,15	23,81
(+) P23396 38S r Ibsom	RSMC2		1,34	0,34		1,08	-0,73	4	4	4	10,8	10,8	10,8	48,632	0	16,291	1507700000	9	P23396;P3	P23396;P3	25,12	25,27	25,00	24,84	24,71	23,88	24,75	24,86	24,97
(+) Q71WX6 ALY-depen	DHX36		1,34	0,43		0,47	-0,74	3	3	3	5,8	5,8	5,8	91,43	0	19,74	80649000	6	Q71WX1;C	Q71WX1;C	22,92	22,86	22,59	23,23	22,03	20,99	22,57	22,14	22,37
(+) Q07200 Heparin-bi	HDGFRP2	+	2,19	2,26	+	1,60	-0,75	5	5	5	11,6	11,6	11,6	74,229	0	24,368	2518100000	17	Q7Z3H5-2;	Q7Z3H5-2;	25,15	24,86	24,63	24,36	24,28	24,12	22,17	22,22	22,00
(+) P80233 L-lactate d	LDHA		0,26	0,27		0,99	-0,75	9	9	9	27,4	27,4	27,4	36,648	0	73,545	11630000000	62	P00338;P0	P00338;P0	25,68	25,80	26,68	25,51	25,39	24,92	25,31	26,25	25,42
(+) Q14980 RNA-bind	RMP31	+	3,00	2,99		0,98	-0,79	4	4	3	18,5	18,5	15,2	34,561	0	15,257	1662500000	26	H0YN90;H	H0YN90;H	23,92	24,18	23,63	24,46	23,27	23,63	21,63	21,25	22,78
(+) H0YB25 3D Glo bo	HDIP1		0,10	0,13		0,74	-0,80	2	2	2	46,8	46,8	46,8	5,3899	0	13,455	1453700000	13	H0Z5L4;M	H0Z5L4;M	22,91	22,89	24,18	22,65	22,30	22,59	23,24	23,13	23,17
(+) Q01540 Scaffold at	SAFB;SAFB	+	1,21	0,29	+	1,79	-0,80	9	9	8	14,2	14,2	14,2	93,18	0	12,183	9581700000	18	Q15424-2;	Q15424-2;	26,72	26,85	26,66	25,56	26,16	26,11	22,69	22,34	22,35
(+) P78316 Eterompin	RTN4R		1,12	-1,68		0,27	-0,80	3	3	3	13,9	13,9	13,9	36,738	0	18,876	2728200000	19	P78316;Q	P78316;Q	21,41	21,59	24,75	24,04	20,79	23,49	19,24	19,54	19,91
(+) Q07564 LIS small s	SMRK1P2	+	1,57	1,19	+	2,15	-0,80	9	9	9	4,5	4,5	4,5	248,5	0	17,467	4122400000	35	Q7Z6K3;Q	Q7Z6K3;Q	25,05	25,26	25,30	24,88	24,55	24,08	24,03	24,31	23,90
(+) Q04637 Heteroge	PTCD3	+	1,27	0,04	+	2,12	-0,84	7	7	7	13,2	13,2	13,2	76,549	0	16,577	5292200000	40	Q96EY7;Q	Q96EY7;Q	25,86	26,21	26,10	25,34	25,39	25,05	20,96	21,11	21,14
(+) P07195 L-lactate d	LDHB		0,97	1,01		0,80	-0,86	8	8	8	20,1	20,1	20,1	36,638	0	69,526	12511000000	31	P07195;C9	P07195;C9	26,67	26,66	27,18	26,32	25,32	25,49	24,78	26,32	25,72
(+) P78344 Eukaryotic	EIF4G2		1,22	1,04		0,94	-0,86	3	3	3	17,9	17,9	17,9	29,221	0	17,436	84662000	5	P78344;P7	P78344;P7	22,99	23,29	23,23	23,29	22,07	22,56	23,03	22,43	21,93
(+) Q13713 Sarcoplasg	EGFL	+	2,29	1,89	+	1,27	-0,86	3	3	3	13,8	13,8	13,8	28,229	0	14,615	2915500000	26	Q8TCJ2;Q	Q8TCJ2;Q	24,90	25,29	24,99	24,21	24,22	23,59	23,16	23,78	23,26
(+) P82932 38S r Ibsom	MRP36		1,86	1,71	+	2,16	-0,90	2	2	2	16	16	16	14,226	0	12,451	1172000000	12	P82932	P82932	24,06	24,14	23,77	23,14	23,20	23,85	22,80	22,53	21,51
(+) P49750 ENA-bind	RMH22		0,24	-0,33	+	1,31	-0,94	3	3	3	5	5	5	100,18	0	17,32	5238400000	15	P49756;M	P49756;	25,29	25,76	25,48	25,19	24,32	24,22	24,39	25,41	25,22
(+) Q13277 Lamina-as	TAPBP		0,03	0,01		0,51	-0,95	2	2	2	6,9	6,9	6,9	46,266	0	16,751	1869900000	12	Q13573;N	Q13573;N	22,24	22,62	23,76	23,21	23,43	23,03	23,38	23,23	23,08
(+) B1AHB1 DNA helic	MCM3	+	1,49	-0,93		0,45	-0,97	7	7	7	14,3	14,3	14,3	77,392	0	42,718	4984400000	18	B1AHB1;P	B1AHB1;P	24,75	24,28	24,60	24,60	21,77	24,27	23,83	25,60	24,98
(+) Q53130 Dehydrog	DHRS2	+	2,63	1,04	+	1,66	-0,97	8	8	8	21,1	21,1	21,1	29,934	0	30,14	10520000000	63	Q53GH8;C	Q53GH8;C	27,17	27,06	26,76	26,34	26,18	25,56	25,83	25,94	26,13
(+) Q05639 Elongation	EEF1A2		0,89	1,88		0,70	-0,99	11	2	2	20,7	7,9	7,9	50,47	0	17,748	2111900000	22	Q05639	Q05639	24,40	23,26	24,46	22,04	22,60	23,23	20,96	21,60	22,93
(+) Q4LJH4 Apoptotic	ACIN1		1,66	4,22		0,89	-0,99	12	12	12	10,7	10,7	10,7	145,44	0	78,187	7432100000	41	Q4LJH4;E7	Q4LJH4;E7	26,02	27,48	25,94	25,71	25,51	25,26	22,07	22,91	21,90
(+) H0YH09 Rab-interm	RCIAP1	+	1,87	2,49	+	1,38	-1,00	6	6	6	10,2	10,2	10,2	80,138	0	43,263	5850800000	33	H0YH09;E	H0YH09;E	25,85	26,08	25,90	24,71	25,60	24,54	23,86	22,93	23,98
(+) P13498 Ribonucle	RNH1		0,23	0,71		0,43	-1,00	2	2	2	6,5	6,5	6,5	49,972	0	14,888	2130400000	18	P13489;E9	P13489;E9	24,15	22,78	24,29	21,80	24,52	22,21	24,26	20,90	24,21
(+) Q01543 Calponin-2	CNN2		0,14	0,11		0,61	-1,02	4	4	4	19,8	19,8	19,8	21,28	0	27,973	2536400000	19	Q15417;Q	Q15417;Q	24,77	24,64	24,27	24,60	23,83	22,09	23,86	24,63	24,74
(+) P51149 2BS r Ibsom	DAP3	+	2,97	3,84		1,15	-1,04	9	9	9	31,5	31,5	31,5	49,044	0	119,74	10030000000	39	P51398-2;	P51398-2;	27,34	27,13	26,73	26,71	26,01	25,27	23,53	23,99	22,55
(+) Q09729 3BS r Ibsom	MRPS22	+	2,05	2,20	+	1,27	-1,04	2	2	2	17	17	17	12,619	0	12,544	1291200000	11	Q9Y399;C	Q9Y399;C	24,11	24,84	23,65	23,23	23,23	23,01	22,45	21,42	22,08
(+) P46821 Transplan	C1744		1,18	0,28		0,66	-1,06	4	4	4	10,9	10,9	10,9	28,024	0	16,172	1592700000	22	P46821;P4	P46821;P4	25,20	25,27	25,13	24,85	25,02	23,76	23,00	25,16	24,78
(+) P31153 Protein S-i	S10147		2,82	-1,89	+	1,94	-1,10	5	5	5	30,7	30,7	30,7	11,471	0	10,913	1263100000	64	P31153;O	P31153;	24,64	25,25	24,98	23,75	24,20	23,63	24,57	27,26	26,61
(+) P15104 Glutamine	MTHFD1	+	1,60	0,61	+	1,25	-1,10	6	6	6	7,1	7,1	7,1	110,61	0	29,921	5525900000	26	P15104;P1	P15104;P1	25,34	25,19	25,20	24,74	24,22	23,46	24,64	24,99	24,55
(+) Q01497 Protein ph	PP31B;A		1,91	2,21		1,28	-1,10	5	5	5	6,4	6,4	6,4	111,18	0	34,224	19150000000	10	Q14974-1;	Q14974-1;	24,47	24,67	24,73	24,01	23,83	22,74	21,47	23,19	22,60
(+) Q08J45 2-Oxoacid	ODO		4,22	15,70		0,57	-1,10	20	20	20	54,4	54,4	54,4	48,063	0	107,94	4,75E+11	459	Q8N4B4;E	Q8N4B4;E	26,44	26,29	26,20	25,75	23,85	23,92	20,69	20,62	19,11
(+) H3BSF1B Rab-like	RAB1A		0,92	-1,28		0,69	-1,12	3	3	3	23,8	23,8	23,8	20,469	0	27,024	1502600000	12	H0FLI6;M	H0FLI6;M	24,08	23,93	22,01	23,97	21,74	20,62	24,19	24,09	23,58
(+) A0A0A	Nucleotr-	NOG1	4,19	2,68	+	1,97	-1,14	11	11	11	13,5	13,5	13,5	74,542	0	75,165	14910000000	60	A0A0A0M	A0A0A0M	27,35	27,81	27,40	25,91	26,76	26,28	24,74	25,07	24,90
(+) P49458 Signal rec	SRP09		0,95	-0,13		0,71	-1,15	3	3	3	20,3	20,3	20,3	10,132	0	14,601	1167700000	15	P49458;E9	P49458;	24,41	24,14	24,26	24,53	22,66	21,89	24,27	24,14	24,28
(+) B3KMD7 GTP-bindi	RAN		1,65	-0,72		0,68	-1,20	4	4	4	23,2	23,2	23,2	26,224	0	25,126	4982400000	32	B3KMD7;E	B3KMD7;E	24,81	24,59	24,91	24,63	23,98	23,72	23,16	25,68	25,70
(+) Q00325 Lemin-B2	LMNB2		1,23	-0,47		1,28	-1,25	7	6	6	11,9	10,6	10,6	69,548	0	28,08	1482700000	27	Q00325	Q00325	23,67	23,84	23,98	23,30	23,63	23,21	24,45	23,99	24,46
(+) P40318 Rac-like	RAB31		2,80	2,28		1,03	-1,41	4	3	3	20,5	15	15	22,541	0	20,221	2068800000	16	P40926	P40926	22,63	24,41	24,36	22,01	23,86	22,20	22,07	21,94	21,55
(+) P27105 Casein kin	CSNK2A1;		1,29	2,80	+	1,74	-1,46	5	5	5	18,7	18,7	18,7	45,31	0	52,661	2896500000	19	P27105;Q	P27105;Q	25,63	25,82	25,73	24,36	24,58	23,90	22,11	22,45	22,13
(+) P53999 Activated	USB1		0,43	0,63		0,91	-1,52	3	3	3	26	26	26	34,291	0	17,104	1296900000	6	P53999	P53999	24,61	24,08	24,02	23,94	21,36	22,91	24,28	22,28	24,14
(+) Q06124 Zinc finger	ZFC3H1		0,67	-0,18		0,21	-1,96	1	1	1	0,9	0,9	0,9	226,35	0,004762	6,1284	10190000000	34	Q6GD50	Q6GD50	26,59	26,46	26,89	21,73	28,15	22,49	31,19	30,15	29,14
(+) A0A087 2BS r Ibsom	MRPS21	+	2,24	2,22		1,04	-1,89	2	2	2	29,9	29,9	29,9	10,688	0	15,889	1588000000	12	A0A075B7	A0A075B7	24,56	24,91	24,28	24,26	21,76	21,98	21,47	22,02	22,27
(+) Q53FI3 Serine/arg	SRSF10;P	+	1,92	2,01		0,74	-1,90	4	4	4	26,2	26,2	26,2	30,913	0	18,064	4267900000	15	Q53FI3;O7	Q53FI3;O7	26,38	26,33	24,49	25,18	24,42	21,99	22,40	22,46	23,21
(+) E9PKJ0 40S r Ibsom	FAU	+	4,13	5,46		0,32	-1,95	2	2	2	11,2	11,2	11,2	11,965	0	12,721	2666600000	16	E9PKJ0;M	E9PKJ0;M	27,80	28,29	27,52	28,32	28,17	20,86	22,58	22,25	21,99
(+) Q04134 Pre-mRNA	DHX15		2,01	4,01		0,91	-1,97	4	4	4	6	6	6	90,932	0	27,222	4139100000	12	Q4G142	Q4G142	25,42	25,67	25,41	22,28	21,86	25,25	23,03	21,29	20,07
(+) Q01734 Tubulin al	TUBA2C;TUBA3E		0,51	1,38	+	1,66	-2,66	13	2	2	41,1	5,3	5,3	49,959	0	15,766	4925500000	25	Q13748;Q	Q13748;Q	25,34	25,40	23,23	22,27	22,00	21,74	22,49	22,36	25,17